N89-20958

WALL INTERFERENCE ASSESSMENT AND CORRECTIONS

P. A. Newman
NASA Langley Research Center
Hampton, Virginia

W. B. Kemp, Jr. and J. A. Garriz
Vigyan Research Associates, Inc.
Hampton, Virginia

SUMMARY

Wind-tunnel-wall interference assessment and correction (WIAC) concepts, applications, and typical results are discussed in terms of several nonlinear transonic codes and one panel method code developed for and being implemented at NASA Langley Research Center. Contrasts between 2-D and 3-D transonic testing factors which affect WIAC procedures are illustrated using airfoil data from the 0.3-m Transonic Cryogenic Tunnel (TCT) and Pathfinder I data from the National Transonic Facility (NTF). Initial results from the 3-D WIAC codes are encouraging; research on and implementation of WIAC concepts will continue.

INTRODUCTION

The technology of wind-tunnel-wall interference was first formulated about 1919 by Prandtl (refs. 1-3), and its continued development, refinement, and extension parallels that of the wind tunnel. The classical theory, taken to mean that based upon boundary value problems for the linearized potential flow equation subject to linearized tunnel-wall boundary conditions, predicted wall interference satisfactorily in the open-jet and solid-wall wind tunnels used for subsonic testing. Furthermore, this theory pointed to the partially open test section as a possibility for minimizing wall interference, prompting the introduction of a slotted wall about 1948 (refs. 4-6). The ventilated wall allowed for tunnel testing through the transonic range without choking; however, for the sensitive high-speed flow and ventilated walls at the test section boundary, flow linearity and homogeneity became suspect. The evolution of this classical wall-interference theory and applications can be traced through a few sample works, listed herein as references 7 to 13.

The introduction of practical high-speed digital computers during the 1960's opened the door to computational aerodynamics. It permitted rapid systematic recalculations of the linear theory wall-interference parameters, particularly those for several formulations of the ventilated-wall boundary conditions (refs. 14, 15). However, interest in obtaining accurate results for the high subsonic speed regime led to the numerical solution of nonlinear partial differential equations. Demonstration of a method for making practical transonic aerodynamic calculations occurred about 1970 (ref. 16) and spawned applications within several years to rather complex geometric configurations and also for more realistic field equation sets. Numerical experiments related to tunnel-wall effects could be performed without the linearization restriction on either the

field equation or the wall boundary condition; it became evident that somewhere in the transonic flow regime linear superposition did not remain valid (ref. 17). During this same time frame, it was realized that ventilated tunnel-wall flow characteristics (from which the wall boundary conditions are obtained) were very nonlinear at transonic flow conditions and dependent upon the model pressure field (ref. 18). Many attempts to obtain satisfactory ventilated-wall boundary conditions have been and still continue to be made (ref. 19, 20); the early history of tunnel-wall boundary conditions can also be traced through the several works listed as references 7 to 13.

The concept of actively adapting the test section wall shape or flow condition in order to eliminate or minimize the interference as the test proceeds was put forward around 1973 (refs. 21, 22). The various procedures for implementing these concepts required hardware complexity in two forms: additional instrumentation for making flow property measurements near (or on) the walls; and, automatically variable geometry for iteratively adapting the test section at each data point. The feasibility of having instrumentation for routinely measuring flow data at or near the walls, as in the adaptive tunnel, also led to reformulations of the classical wall-interference ideas where various measured data were used in lieu of tunnel-wall and/or model boundary conditions. Two such posttest wall-interference-assessment formulations for 2-D subsonic and transonic flow were given in references 23 and 24, respectively; in these two, only measured pressures are used in the boundary conditions. Most posttest wall-interference-assessment/correction (WIAC) procedures were formulated by the early 1980's and are based upon linear field equations. However, since this is a transonic symposium, the present discussion of WIAC emphasizes the nonlinear transonic procedures. Progress in developing and applying WIAC methods from the mid-1970's to the present can be traced through the topical conference proceedings and summary papers listed as references 25 to 35.

In this paper, WIAC concepts, applications, and typical results are discussed in terms of several nonlinear transonic codes (refs. 23, 24, 36-48) and one panel method code (refs. 49-51) developed for and being implemented at NASA Langley Research Center. Contrasts between 2-D and 3-D transonic testing factors which affect WIAC procedures are illustrated using airfoil data from the 0.3-m Transonic Cryogenic Tunnel (TCT) and Pathfinder I data from the National Transonic Facility (NTF). In addition, both 2-D and 3-D Euler equation method WIAC codes have been developed (refs. 52, 53) but not yet implemented into a procedure nor used on real wind-tunnel data; the 3-D code is briefly discussed. The nonlinear procedures discussed herein are truly representative of what is currently available; only five other nonlinear code procedures have been published and apparently none of them has been used very much. Of these latter procedures, three are for 2-D flow (refs. 54-56), another is for axisymmetric flow (ref. 57), and the last is a two-variable procedure for 3-D flow (ref. 19). Note that reference 56, which discusses the latter of these 2-D nonlinear procedures, is the following paper in these proceedings. The 2-D WIAC procedures are pretty mature; a few sample results are shown and general observations about applications are made. Results from application of 3-D nonlinear transonic WIAC procedures to real wind-tunnel data have not yet been published; however, limited initial results for the Pathfinder I model tested in the NTF are given herein. Other research groups in government and industry have contributed to developing and testing the nonlinear WIAC procedures which are discussed.

SYMBOLS

arabic

b	wing or airfoil semispan
c	airfoil chord
$\bar{c}$	wing mean chord
C_d	2-D or section drag coefficient
C_ℓ	2-D or section lift coefficient
C_L	3-D configuration lift coefficient
C_m	2-D or section moment coefficient
C_n	2-D or section normal force coefficient
C_p	pressure coefficient
h	tunnel half-height
M	Mach number
Re	Reynolds number
Re_c	Reynolds number based on chord
u,v,w	velocity components parallel to x,y,z
v_{up}	vertical velocity at upstream end of test section
x, y, z	Cartesian coordinates, x streamwise

subscripts

c, corr	corrected condition or at corrected conditions
ref	reference condition or at reference condition
t	tail
w	wing
T	tunnel condition
WI	classical wall interference correction
WIAC	wall interference assessment/correction
o	calibration condition

greek

α	angle of attack
ΔC_p	pressure coefficient difference
ΔM	Mach number correction, = $M_{corr} - M_{ref}$
$\Delta\alpha$	angle-of-attack correction, = $\alpha_{corr} - \alpha_{ref}$
$\Delta C_{p_{wall}}$	scatter in wall pressure coefficient measurements
$\Delta C_{p_{gauge}}$	error due to pressure gauge accuracy
θ	flow angularity, = v/u
τ	airfoil thickness to chord ratio

abbreviations

AR	Model Aspect Ratio
AW, AWTS	Adaptive-Wall Test Section
BC	Boundary Condition
CFD	Computational Fluid Dynamics
DFVLR	Deutsche Forschungs- und Versuchsanstalt für Luft- und Raumfahrt
EUCOR3D	3-D Euler Equation WIAC code
NACA	National Advisory Committee for Aeronautics
NASA	National Aeronautics and Space Administration
NTF	National Transonic Facility
PANCOR	3-D Panel Method WIAC code
SW, SWTS	Slotted-Wall Test Section
SWBL	Sidewall Boundary Layer
TUNCOR	3-D TSDE Method WIAC code
TCT	Transonic Cryogenic Tunnel
TS	Test Section

TSDE	Transonic Small Disturbance Equation
VLOR	Vertical Line Over-Relaxation
WBT	Wing-Body-Tail Configuration
WIAC	Wall Interference Assessment/Correction
1-D	One-dimensional
2-D	Two-dimensional
3-D	Three-dimensional

WIAC CONCEPT, METHODS AND VALIDATION

WIAC concepts and applications draw upon ideas and capabilities from classical wall-interference theory, computational fluid dynamics (CFD) capabilities, and adaptive-wall technology. Briefly stated, the WIAC concept is to determine the wall interference which exists in conventional or partially adapted wind-tunnel data by making use of measurements made during the test, generally at or near the test-section walls. WIAC is, therefore, a posttest technique. The various applications or realizations of it depend upon the amount and type of data taken, the fluid flow equation approximations used in the analysis, the tunnel geometry and capabilities, as well as the timeliness, costliness, and accuracy desired in the result. It is not expected that all test data can be corrected; an assessment procedure should give some indication of the measure of goodness for the corrections which are obtained. When one considers the trade-offs between computational complexity versus wind-tunnel complexity, the two extremes being complete 3-D Navier-Stokes CFD solutions and 3-D adaptive-wall wind-tunnel data, respectively, then WIAC techniques lie between those extremes, hopefully making good use of the best practical aspects of both computational and wind-tunnel simulations.

Traditionally, transonic testing of both 2-D airfoil and 3-D configuration models has been carried out in wind tunnels with ventilated-wall test sections. As already noted, the flow interactions at these finite length walls are generally neither homogeneous nor linear and can be greatly influenced by the model flow field. Thus it is not surprising that the classical linear theories were found to be inadequate. For wind-tunnel data taken in most 3-D transonic facilities with ventilated-wall test sections, no wall-interference corrections were made. The renewed interest and effort in transonic wall-interference corrections here at NASA Langley commenced about 1974 in order to support the NTF. In this facility where both Mach and Reynolds numbers of free flight could be simulated (ref. 58, the first paper in this proceedings), wall interference would be a prime candidate for uncertainty in the test data. A conventional slotted-wall test section (with some capability to vary test-section divergence angle, reentry flap angle and step height, and diffuser entrance angle) was chosen since the 3-D adaptive wall concept had not yet been demonstrated to be feasible. Reference 59, a prior paper in this proceedings, discusses the history and current status of adaptive wall wind-tunnel technology. The total wall-

interference assessment/reduction effort at Langley which resulted from this renewed interest sparked by NTF was summarized in reference 33.

The elements involved in establishing the corrected test conditions in conventional transonic wind tunnels are depicted in Table I. Calibration runs and flow-angle surveys will have been made to determine the tunnel-empty Mach number and angle-of-attack offsets at the model location (ΔM_o, $\Delta\alpha_o$) which are to be applied in the data reduction process to reference conditions (M_{ref}, α_{ref}) for each test-data point in order to obtain the tunnel test conditions (M_T, α_T). Wall interference corrections in the conventional sense (ΔM_{WI}, $\Delta\alpha_{WI}$) are then determined by some procedure or analysis and applied to obtain the corrected flow conditions (M_c, α_c). As previously noted, this latter step is frequently not taken with ventilated transonic tunnel data. WIAC was developed and pursued in order to be able either to perform this latter step in a consistent and meaningful way or to indicate that it might not be possible. However, it should be pointed out that WIAC is not limited to application at only the latter step, as will be shown subsequently. The last entry in Table I is intended to indicate that the WIAC quantities (ΔM_{WIAC}, $\Delta\alpha_{WIAC}$) may be obtained with or without regard to a tunnel calibration and applied to whatever flow conditions ($M_?$, $\alpha_?$) were quoted as belonging to (i.e., used to reduce) the test data. In fact, application of WIAC procedures to calibration run data provides information about the tunnel-empty flow and effects due to variable tunnel-geometry parameters (ref. 51). For adapted-wall or partially adapted-wall tunnels, it is not clear what meaning should be attached to the tunnel-empty calibration. The WIAC procedure can be constructed to model (account for) tunnel geometry other than just the constraining walls (i.e., sting, sting support, etc.); the corrections obtained are then more properly called tunnel-interference rather than simply wall-interference corrections.

Transonic Concept

As previously noted, the possibility of routinely measuring flow data at or near the test-section walls (as required in the adaptive-wall tunnel) led to reformulations of the classical wall-interference ideas for 2-D airfoil tunnel data at subsonic (ref. 23) and transonic (ref. 24) flow conditions. A schematic of the WIAC concept where pressure measurements are made on both the top and bottom test-section walls as well as on both model surfaces is shown in Figure 1. As shown on the left side, the tunnel is instrumented to make the additional wall measurements. As shown on the right side, one now solves at least two fluid flow problems. The first is an equivalent inviscid tunnel flow simulation where pressure measurements on the walls and the model are specified boundary values with the measured lift and drag forces constrained (i.e., also used or matched). Since this is an inverse (or design-like) problem, the equivalent inviscid model shape is obtained as its solution. This shape is then used as the internal boundary condition in the second problem, with external boundary conditions appropriate to unbounded flow (free air). In this solution, the far-field Mach number, M, and angle of attack, α, required to minimize the error in local velocity (squared) or Mach number over the airfoil surface between these two calculated solutions are determined. The adjustments to far-field Mach number and angle of attack so determined define the corrections to tunnel conditions and the value of the error which was minimized is a measure of the residual interference.

In Figure 2, the upper half-plane of a Cartesian grid used in the transonic 2-D WIAC (ref. 24) is shown. The wind-tunnel grid (outlined by the inner bold lines) is used in the first problem discussed above; it is a proper subset of the free-air grid used in the second problem. The top and bottom wall boundary conditions are derived from the measured tunnel-wall pressure coefficients, C_p, and enforced along grid lines at the (mean) tunnel-wall location. Lift and, indirectly, drag enter the downstream outflow boundary condition, whereas it was assumed that the upstream upwash velocity components v_{up} near the walls would be measured and used in the inflow boundary condition. However, it was found (ref. 38) that these upwash components could be obtained iteratively by successive passes through the WIAC code if they were not measured. The airfoil boundary conditions, C_p for the in-tunnel calculation and equivalent inviscid airfoil shape for the free-air calculation, are applied along the slit as noted on Figure 2. For the free-air calculation, the grid extends outward in all directions from the tunnel grid, and approximate free-air far-field boundary conditions are imposed.

Classification of Methods

Kraft (ref. 60) has categorized WIAC procedures in terms of the number of measured data arrays used in the boundary conditions. The zero (0) measured-data array procedures are, therefore, pretest procedures and include the classical wall-interference correction methods as well as a number of more recent CFD code analyses which implement the tunnel-wall boundary condition in some functional (or empirical) form. The one (1) measured-data array procedures utilize one flow-variable array (C_p or θ or u or v) measured along an interface near (or on) the wall as outer boundary data. The two (2) measured-data array procedures utilize either two flow-variable arrays (C_p and θ or u and v) measured along an interface near (or on) the wall or one flow-variable array measured along two interfaces or boundaries. For 2-D WIAC procedures, these arrays of measured data are 1-D whereas for 3-D WIAC procedures the arrays are 2-D on each interface.

The concept outlined on Figures 1 and 2 applies to the 2-D transonic small disturbance equation (TSDE) WIAC procedures developed (refs. 23, 24, 36-44) and used to obtain the sample results to be presented herein; it is seen to be one type of the two-measured flow-variable array procedures. Another of this type, but using θ rather than C_p, was described by Schairer (ref. 61). Other 2-D WIAC procedures utilizing the two measured-variable arrays on one surface for boundary specification have been described by Ashill and Weeks (ref. 62), by Kraft and Dahm (ref. 63), and, at this symposium, by Lo and Sickles (ref. 56). These methods need no a priori definition of either the test model or the tunnel-wall characteristics. The 2-D WIAC procedures utilizing one measured-variable array at the walls (e.g., static pressure) plus a model representation based on known model geometry and aerodynamic loads have been given by Capelier, Chevallier, and Bouniol (ref. 64), Sawada (ref. 65), Mokry and Ohman (ref. 66), and Smith (ref. 67). Methods using either of the above boundary types require the assumption of linear superposition of model and tunnel influences to quantify the tunnel interference and, therefore, are strictly applicable only to purely subsonic flows. They are probably suitable, however, for low transonic cases where the outer boundary flow is fully subsonic. A review of most of these 2-D procedures is given in reference 31.

Both of the 3-D WIAC procedures developed (refs. 45-51) and used to obtain the sample results to be presented herein are one measured flow-variable array procedures. Measured tunnel-wall C_p data are used in the outer-wall boundary condition but the model is defined by its real geometry. For the 3-D TSDE WIAC procedure, TUNCOR, the inner model boundary condition for both the in-tunnel and free-air calculations is the model shape. With this one important exception, the TUNCOR concept and method are 3-D analogs of that outlined in Figures 1 and 2. For the 3-D panel method WIAC procedure, PANCOR, the measured wall C_p data are used in conjunction with geometric data (related to the slotted wall, plenum, and reentry flaps) to define the complete outer-wall boundary condition, as will be discussed later. The Euler equation based WIAC code (ref. 53) mentioned later is also a one measured-variable array method utilizing C_p in the outer boundary condition. Other 3-D one measured-variable array linear procedures have been developed by Rizk and Smithmeyer (ref. 68), Mokry (ref. 69), Schulz (ref. 70), Labrujere (ref. 71), Moses (ref. 72), and Crites (ref. 73), for example. Two 3-D two measured-variable array procedures have been discussed by Schairer (ref. 74) and Kraft, et al. (ref. 19). The classification by Kraft (ref. 60) does not distinguish those procedures which have been formulated to include the nonlinear flow equations; in fact, many of the WIAC procedures rely on linear superposition and are, therefore, not strictly appropriate for flows with extensive regions of supercritical flow. The nonlinear procedures to be discussed and others which are available have been identified in the Introduction section of this paper.

Validation Procedure

Validation or verification of the WIAC procedure results (or, for that matter, those obtained by any means) must depend upon the mutual agreement or consistency of results from all viable means of obtaining the answer. Since the WIAC is both an assessment and correction procedure, it is natural to assume that all test data contain some wall interference. Operating from this premise then, one would expect to obtain consistent corrected results for data from separate tests of a common model shape if the WIAC procedure were valid in accounting for all pertinent aspects of the interference. That is, test data on the same model in different tunnels/test sections, or test data from different size models in the same facility should collapse to a common curve, result, etc. A second variation of this theme is to make independent free-air flow-field calculations with the best available CFD codes at both uncorrected (M_T, α_T) and corrected (M_{corr}, α_{corr}) flow conditions. Comparison of calculated detail results (such as model surface C_p, lift-curve slope, drag-rise Mach number, etc.) with the experimental data and the experimental data renormalized to the corrected conditions, respectively, allows one to ascertain whether or not the corrections are valid or, perhaps, the range of validity.

WIAC APPLICATIONS TO AIRFOIL (2-D) DATA

Initial applications of WIAC were to airfoil tunnel data where, to good approximation, the flow is 2-D. Most of the procedures, both linear and nonlinear, have been discussed in reference 31. The techniques are relatively mature, but questions still remain concerning the tunnel sidewall boundary-layer (SWBL) interaction, particularly at transonic flow conditions. In this section,

test techniques which affect WIAC for 2-D transonic airfoil tunnel data are discussed so that a comparison can be made with the 3-D case. Then, recent results from application of nonlinear WIAC to sample data from the 0.3m TCT are given to illustrate several points.

2-D Test Techniques Affecting WIAC

Table II gives the transonic testing factors affecting 2-D WIAC. For routine testing, the airfoil chord, c, is typically the order of 1/2 to 1/4 of the tunnel half-height, h, resulting in solid blockage ratios, $\tau/(2h/c)$, of several percent. The measured model data generally includes 1-D pressure data, C_p, with good resolution which can be integrated to produce good values for the normal force coefficient, C_n, and moment coefficient, C_m. The drag coefficient, C_d, is normally deduced from measurements of the wake momentum deficit, taken on a wake rake. It is deemed to be more accurate than the value obtained using the axial force from integrated model pressures along with α_T and C_n. Measured field data on an interface near (or on) the upper and lower walls are needed for WIAC. These 1-D arrays are taken very near the center of the walls; C_p data can be obtained with good resolution and signal (to noise) strength. Figure 3 shows distributions of C_p (negative up) on the airfoil and tunnel walls. These data were from the 0.3-m TCT slotted-wall test section with a nominally sized (h/c = 2.0) supercritical model at transonic flow conditions. The vertical scale is given as the pressure coefficient difference, ΔC_p, over the vertical length of the chord, c. It can be seen that both on the model and wall the pressure signal (to noise) strength is good.

Measurements of 1-D data arrays of the flow angularity, θ, or upwash velocity, v, are more difficult near the walls of the ventilated-wall test sections used for transonic testing. In the case of the solid-wall adaptive tunnels, this information (within the local viscous effect) is given by the wall location. With all WIAC procedures using one-variable arrays of C_p or u, one flow angularity or upwash velocity measurement is required; it is needed by WIAC as an integration constant. In the present 2-D nonlinear WIAC procedures, this requirement has been circumvented in second and succeeding WIAC passes by using the front portion of the airfoil as a flow angle probe; procedures using two measured-variable arrays on a single interface should not require the additional θ measurement.

In airfoil testing, models are mounted between the two sidewalls on turntables in order to provide angle-of-attack changes. The boundary layers on these two sidewalls (SWBL) are subjected to the model pressure field which includes severe adverse pressure gradients (for the flow approaching the model leading and trailing edges and at shock waves) and rapid favorable gradients (behind the model leading and trailing edges). These SWBL interactions become so severe at transonic high-lift conditions that the flow is no longer 2-D. In fact, there are always some manifestations of 3-D flow near the sidewalls. This present 2-D nonlinear WIAC procedure incorporates several simple means for approximating the subsonic attached-flow SWBL interaction due to Barnwell and Sewall (ref. 75) and Murthy (ref. 76). Transonic 2-D WIAC procedures must include some accounting for the SWBL interaction; i.e., a 4-wall correction.

The test section design of ventilated-wall airfoil tunnels is generally near the classical-theory minimum blockage condition; this is required in order to be able to test without choking or extremely large blockage (Mach number) corrections. The test sections are ventilated, either by means of holes (perforated) or longitudinal slots. The minimum blockage condition, however, does mean that large angle-of-attack corrections are to be expected according to classical wall-interference theory. Adaptive-wall test sections have been used now for about a decade (ref. 59) in pilot-size (less than 1-ft diameter) and small (~2-ft diameter) airfoil tunnels. In these facilities, the wall adaptation attempts to minimize all aspects of the wall interference. The present adaptive-wall nonlinear 2-D WIAC procedure is deemed to assess and correct for the residual interferences.

Sample Results for 0.3-m TCT Data

A number of results obtained from various versions of the nonlinear 2-D airfoil WIAC codes have been presented over the last few years in references 23, 24, and 36-44. These results have been for data obtained in the NASA Langley 0.3-m TCT (ref. 77) for several different airfoil shapes tested during the Advanced Technology Airfoil Test Program (ref. 78) and later cooperative agreements with industry and foreign government laboratories. WIAC results have been obtained for both slotted- and adaptive-wall test sections. The technology is mature, and several findings have evolved from the work. These are briefly summarized as follows:

(a) For all of the airfoil data assessed to date, some wall interference appears to be present according to the WIAC procedure.

(b) The SWBL interaction effects appear to be part of (sometimes dominating) this wall interference and must be accounted for in WIAC.

(c) For test conditions near and above the transonic drag rise for aft-loaded supercritical airfoils at moderate to high lift, the simple approximate SWBL interaction models are inadequate (which is not surprising since these models are based upon subsonic attached-flow theories).

(d) Multiple passes (2 or 3) through the WIAC procedure are required to properly assess the unmeasured upstream flow angularity which directly influences the angle-of-attack correction.

(e) WIAC results for both ΔM and $\Delta\alpha$ are smaller for the adapted-wall test section than those for the slotted-wall test section.

(f) Independent transonic free-air CFD code solutions from both conservative full-potential with interacted boundary-layer (ref. 79) and Navier-Stokes (ref. 80) tend to confirm the WIAC results, except as noted in (c) above.

(g) Corrected data for common airfoils tested at different size and in different test sections tend to collapse to a common curve; i.e., the corrected data correlates.

(h) Not all test data are correctable by WIAC; for some cases the code solutions may not be obtained and for others, there may not be a good correspondence with any free-air result. Quantitative interpretation of the WIAC measure of error still appears to be elusive.

Some of the findings summarized above concerning application of the 2-D nonlinear WIAC are illustrated on the next several figures using transonic data for two different airfoils. Sample data and WIAC results for NACA 0012 airfoils of three chord lengths and CAST 10-2/DOA 2 airfoils of two chord lengths are discussed. The relative sizes of the models with respect to the test sections in which they were tested are given in Table III; also indicated are tunnel half-height to chord ratios, model aspect ratios, model thickness ratios, and references for both the data and WIAC results. As indicated earlier in discussing the present transonic WIAC concept, both the measured lift and drag are constrained; therefore, corrections to Mach number and angle-of-attack generally produce only small changes (due to the dynamic pressure rescaling) in C_ℓ and C_d, C_d being measured via the wake rake. Thus, the angle-of-attack correction, $\Delta\alpha$, is seen on a lift curve plot (C_ℓ versus α) as an α shift at almost constant C_ℓ whereas the Mach number correction, ΔM, is seen on a drag rise plot (C_d versus M) as an M shift at almost constant C_d. For a ventilated 2-D airfoil tunnel designed at near minimum classical blockage, the Mach number correction is generally small up to near the drag rise Mach number and above unless the contribution from the SWBL effect is large.

Shown in Figure 4 are the results of applying the 2-D WIAC to data from the adaptive-wall 0.3-m TCT for two different size models. The data shown were obtained during the adaptation sequence from unadapted to fully-adapted. These are lift curve plots and therefore illustrate the corrections to angle-of-attack at the nominal test conditions of M_T=0.65, $\alpha_T = 2^\circ$, and $Re_c = 9\times10^6$ on two different size NACA 0012 airfoils, h/c = 1.0 and h/c = 0.5. Data are shown as symbols for seven different model/tunnel configurations (though not all distinguishable at this scale) and these represent seven different tunnel wall interferences. The uncorrected data are shown in the upper left hand plot, having different C_ℓ at the same nominal test α. The solid curve, shown on all plots in this figure, is the free-air Navier-Stokes solution obtained from the code of Swanson and Turkel (ref. 80). The first application of WIAC (1st pass) assumes that the far upstream flow direction at the upper and lower wall positions is known and is used in the upstream boundary condition. As can be seen in the upper right hand plot, the angle-of-attack correction makes the lift-curve slopes for the two models approximately the same, but the curves themselves appear to have been displaced from one another. Successive applications of the WIAC procedure (passes) with improving estimates of the upstream flow direction (as deduced from the alignment of the computed and real model camber lines) produce angle-of-attack corrections which tend to collapse the two sets of data around the Navier-Stokes free-air solution. The interference and thus corrections were greatest for the larger model (h/c = 0.5, the 13" chord model in the 13" high AWTS) at the highest lift level; three WIAC passes were required to produce an acceptable correction.

The results of applying the 2-D WIAC to data from the slotted-wall test section of the 0.3-m TCT for two different size CAST 10-2/DOA 2 airfoils are shown in Figure 5. These are drag-rise curves and thus illustrate the Mach number corrections which are directly related to the SWBL interference and our approximation of it. The uncorrected data, plotted at the left, shows distinctly different drag-rise Mach numbers for the two different size models. Application of WIAC with the Barnwell-Sewall (ref. 75) SWBL approximation produces Mach number corrections which tend to spread, rather than collapse the curves at the drag rise as shown in the center plot. The Murthy (ref. 76) SWBL approximation includes a model aspect-ratio factor and reduces to the Barnwell-Sewall

approximation in the limit AR → 0, a narrow tunnel. It can be seen in the plot at the right that the knee of the drag-rise curves are most nearly collapsed, tending to define the same drag-rise Mach number.

Shown in Figure 6 are the results of applying the 2-D WIAC to data for the NACA 0012 airfoil in several sizes from both slotted-wall and fully adapted-wall test sections of the 0.3-m TCT. Both uncorrected and corrected data for lift curves (C_ℓ vs. α) and drag-rise curves (C_d vs. M) are shown in Figures 6a and 6b, respectively. The free-air Navier-Stokes results shown as the solid line are obtained from the code described in reference 80. The WIAC results utilized the SWBL approximation of Murthy (ref. 76). Again, the corrected data are collapsed and correlate well with the free-air result at the corrected conditions. Note also that the angle-of-attack and Mach number corrections are larger for the slotted-wall data.

WIAC APPLICATIONS TO CONFIGURATION (3-D) DATA

There are several fundamental differences between 2-D and 3-D transonic testing techniques and practices which have important implications for the WIAC procedures. Two of these differences are the amount of data measured and the means of model support. These will be discussed for the 3-D case in the following section and contrasted with the 2-D case discussed previously.

As already mentioned, several applications of linear WIAC procedures to 3-D tunnel data have appeared in the literature. The 3-D nonlinear WIAC results shown in the last section here, for the Pathfinder I in the NTF, are the first such results, as far as we know, to be published.

3-D Test Techniques Affecting WIAC

Table IV gives the testing factors affecting 3-D WIAC. Typical model sizes for transonic testing are generally governed by the model wing span, 2b, lift level, or body length. This results in solid blockage ratios of 1/2 to 1 percent; i.e., much less than 2-D airfoil tunnels. Thus, wing-section chord lengths are less than those in 2-D tunnels, and even when pressure distributions are measured, the resolution is not as good. Furthermore, there are seldom more than a few chordwise rows of pressure taps so that the resulting 2-D C_p arrays on the model are indeed very sparse. In fact, for many tests no model surface pressures are taken. For most tests, force balances are installed in the model or sting mount so that model aerodynamic forces are available. Thus, most 3-D WIAC procedures are constructed assuming that model pressures will not be available to be used as an inverse internal boundary condition. The model description must come from its geometry and the measured forces if it is required by the WIAC procedure. Figure 7a shows typical wing pressure coefficient data from the Pathfinder I model in the NTF. The dashed lines in the C_p distribution indicate missing data at the leading and trailing edges. Where data are taken, on six spanwise wing stations in this case, as indicated at the left, the signal (to noise) strength is good.

Measured 2-D field data arrays on interfaces near (or on) all walls are generally required by the 3-D WIAC procedures. Such large amounts of data are not going to be taken routinely and even those data which are taken generally have small signal (to noise) strength. This is illustrated in Figure 7b, where NTF wall pressure data, taken for a Pathfinder I test point, are shown along the top, bottom, and sidewall centerlines. As indicated at the left, the top and bottom wall data are taken on the centerlines of three slats, whereas the two sidewall pressure tap rows off the centerline are in the solid blanks covering the region reserved for the sidewall slots. The 2-D data arrays are indeed sparse, and the "noise" is evident; more will be said about this aspect later.

Measurement of 2-D arrays of the flow angularity, θ, or boundary interface normal velocities near the walls is extremely difficult. The small blockage coupled with the 3-D relief effect implies very small signal strength. Thus the present 3-D WIAC procedures do not rely on such arrays of flow data. However, several simultaneous flow angularity measurements or frequent model inverted runs may be required in order to properly assess the upstream flow angularity which effectively appears in the boundary data or as integration constants.

The model support effects and resulting interference in 3-D testing are varied, depending on both the facility and test data desired. In semispan model testing there is generally one SWBL interaction at the root station. For transonic flow conditions where shock waves impinge upon this SWBL, the true 3-D effects are modified. In the WIAC procedure, measured C_p data, rather than a symmetry condition, should be used for the mounting-wall boundary condition. The usual means for supporting full-span models is a sting at the rear of the model generally through the fuselage. The model support can also be done via blade mount into the fuselage bottom or from the top at the vertical tail. These latter two arrangements, as well as some high angle-of-attack testing, require more complicated bent stings. The support interference can thus differ from test to test and, even though not generally considered to be wall interference, is certainly part of the tunnel environment interference. At transonic flow speeds, one may not be able to decompose or separately account for all of the individual interferences; therefore, the concept of tunnel interference may be the most proper.

Design criteria for 3-D transonic test sections vary even though most of the conventional ones are now ventilated. Again the relatively small blockage and 3-D relief effects make the classical minimum blockage criteria of lesser importance than in the airfoil tunnel. Adaptive-wall test sections specifically designed for 3-D testing have been at the pilot-size, with the one exception being the "rubber-wall" subsonic tunnel of the DFVLR (ref. 59). Several 2-D adaptive-wall tunnels have been used for testing 3-D models (ref. 59), and the criterion to which the 2-D wall is adapted varies. In these latter facilities, there will surely be residual interference, for which one needs a 3-D WIAC procedure. The two measured-variable array WIAC procedures may be better suited for this task. The last paper in this symposium (ref. 85) gives results for a semi-span wing tested in the 2-D AWTS of the 0.3-m TCT.

Description of 3-D Codes

Some features of the 3-D WIAC codes being developed for use in the NTF and to be discussed here are given in Table V. The left column lists the code

characteristics to be covered whereas the next three columns give those characteristics for the WIAC codes PANCOR, TUNCOR, and EUCOR3D respectively. PANCOR is based on linear-theory panel methods whereas TUNCOR and EUCOR3D are based on nonlinear flow equations.

The PANCOR code was developed by Kemp (refs. 49-51) in order to simulate the slotted-wall boundary flow features better than would be possible by using only the sparsely measured C_p distributions alone. Figure 8 depicts the types of singularity panels and networks used in PANCOR for the tunnel boundaries. It can be seen that the finite length, discrete, segmented source lines are used to simulate the slots; their strength is governed by the sparsely measured slotted-wall C_p distributions. Panel representations are used to simulate the solid surfaces (slats between the slots, sidewalls, and reentry flaps) as well as to enforce unperturbed outer flow and flow through the end planes of the test section. In addition, other tunnel features such as variable wall divergence, reentry flap settings, model sting, and sting support sector are also treated in PANCOR. Sample results from the application of this code to NTF data are shown later.

The TUNCOR code was developed by Rizk, et al (refs. 45-48) in order to provide a (nonlinear) transonic WIAC capability for the NTF. As indicated in Table V, this code is based upon numerical vertical line overrelaxation (VLOR) solutions of 3-D TSDE's, analogous to the 2-D procedure previously discussed. The grid and boundary conditions are the 3-D extensions of those depicted for the 2-D WIAC in Figure 2. The sparsely measured C_p distribution data on all of the walls are enriched and interpolated onto the outer boundary grid for the tunnel flow calculation in the WIAC procedure. Sample results from the application of this code to NTF data are also shown later.

The EUCOR3D code was also developed by Rizk et al (refs. 52, 53) in order to overcome some of the approximations inherent in the TSDE formulation of TUNCOR and to provide benchmark corrections against which more approximate WIAC codes could be evaluated. As indicated in the right column of Table V, EUCOR3D is based upon the Euler equations which are solved by an efficient numerical algorithm on an H-H body fitted grid. Figure 9 depicts this grid for a wing-body configuration; both symmetry plane and spanwise section cuts through the grid near the model are shown; the final shearing transformations to the outer flat tunnel-wall boundaries have not been included here. This code is still being debugged and adapted into a partially automated procedure; it has not yet been applied to real tunnel data.

Sample Results for NTF Data

WIAC results relevant to the NTF which are discussed here include numerical simulations of the Pathfinder I model in NTF-sized ideal tunnels, assessment of the "tunnel-empty" interference using NTF calibration data, and initial corrections of Pathfinder I data taken in the NTF. The size of the Pathfinder I model with respect to the NTF was that of a typical transport configuration for testing at high-subsonic speeds with little wall interference according to conventional guidelines. It was a 0.5% solid-blockage model. The only data published to date for both the NTF calibration and Pathfinder I tests are given in reference 58, the first talk in this symposium.

Numerically Simulated Pathfinder I in Ideal Tunnels

Numerical simulation of the Pathfinder I model in NTF-size ideal tunnels was performed in order to bracket and size the wall-interference corrections to be expected in the NTF. The open-jet and solid-wall outer boundary conditions represent the two extremes of a slotted-wall and, according to classical 3-D wall interference theory, produce corrections ΔM and $\Delta\alpha$ which bracket those for the ideal slotted wall. The numerical simulations were carried out using various options of the TUNCOR 3-D WIAC procedure; values of ΔM and $\Delta\alpha$ which were obtained are given in Table VI. The NTF test section design criterion was to eliminate lift interference with all four walls slotted, according to an empirically correlated ideal slotted-wall theory (ref. 86). Currently, the NTF sidewall slots are closed; therefore, the current configuration should appear to be somewhat closed. It can be seen from Table VI that the numerically simulated open-jet and solid-wall test section results bound those for the NTF slotted-wall configuration which were obtained from classical theory. This classical theory calculation also shows the present NTF configuration to be somewhat closed.

Figure 10 illustrates the effect of the WIAC corrections for these ideal open-jet and solid-wall tunnel results, in particular, those for the flow parameters C_L and the size of the embedded region of supersonic flow above the wing. The simulated test conditions are $M_T = 0.82$ and $\alpha_T = 1.93^\circ$. The lift curve, shown in Figure 10(a), is not sensitive to the Mach number correction, ΔM, so the effect of the angle-of-attack correction, $\Delta\alpha$, is readily seen. The baseline free-air curve, over approximately a 0.6° range, is established by the three open circles connected by the solid line; the open-jet and solid-wall tunnel solutions at the nominal α_T are seen to lie below and above the free-air curve, respectively. When the WIAC is applied, these results are shifted by $\Delta\alpha$ as indicated and lie very near the free-air curve. Figure 10(b) is more complicated since the size of the embedded supersonic flow region (bubble) depends upon both M and α (ΔM and $\Delta\alpha$). The free-air solution surface for this parameter versus M and α is denoted by the five open circles connected by solid lines, traces for $M = M_T$ (with α variable) and $\alpha = \alpha_T$ (with M variable). At the nominal tunnel conditions, M_T and α_T, the open-jet and solid-wall tunnel results lie below and above the free-air surface respectively. Upon correction by the WIAC procedure, the results are seen to closely approach the free-air surface from below and above, respectively.

Typical NTF Calibration Data

Recall from the earlier discussion on the WIAC concept that calibration tests are performed to assess the "tunnel-empty" Mach number, ΔM_o, and flow angularity, $\Delta\alpha_o$, offsets (corrections) which must be applied to the reference values deduced from the measured data in order to arrive at the test conditions, M_T and α_T. Conventional wall-interference corrections, ΔM_{WI} and $\Delta\alpha_{WI}$, are then deemed to be those attributable to the wall <u>after</u> consideration of the calibration offsets. The WIAC procedure can be applied with or without the calibration; however, some subtle differences need to be considered. Kemp (ref. 51) has discussed the philosophy of WIAC without regard to needing the tunnel calibration, structured the PANCOR procedure accordingly and, thus, obtains tunnel corrections (or more properly, interference fields) which correspond to ΔM_{WI} and $\Delta\alpha_{WI}$ <u>plus</u> the effect of calibration offsets.

In the NTF, test-section wall-divergence (convergence) angles can be varied in order to provide the capability for maintaining zero Mach number gradient through the "empty" test section over the wide range of Mach and Reynolds numbers achievable. Typical wall-angle settings for uniform tunnel-empty Mach number through the test section as well as the Mach number offsets (corrections) from the reference values are determined in the tunnel calibration as a function of M and Re. During this calibration, wall pressure data were taken so that the WIAC codes could be used to assess the calibration. Application of WIAC procedures to calibration data provides information about the tunnel-empty flow and effects due to variable tunnel-geometry parameters. Such studies have been made using the PANCOR code and are reported in reference 51. An example of the PANCOR WIAC analysis for two sample NTF calibration points is shown in Figure 11. The distribution of flow angle along the tunnel centerline is shown. The upstream test-section flow angularity was assumed to be zero and, according to the WIAC code, a downwash is being produced which amounts to about 0.1° at the nominal model location. This occurs for both $M_T = 0.6$ and 0.8.

Results from both TUNCOR and PANCOR WIAC analyses of calibration data from the NTF for nominal tunnel Mach numbers of 0.6 and 0.8 at a Reynolds number of 4×10^6/ft are given in Table VII. Here, the WIAC results are compared with the experimental values of ΔM from the tunnel calibration and $\Delta\alpha$ obtained from lifting models tested in both the upright and inverted positions (ref. 58). The first row of results (where the upstream upwash velocity, v_{up}, is set to zero) is from the first pass. Both WIAC codes assess, from the measured wall-pressure signatures used in the boundary conditions, that the upstream part of the test section is generating about 0.1° downwash, indicating either (a) that value at the model position, or (b) a non-zero upwash at the upstream end of the test section. As can be seen from the model upright and inverted tests, the flow angularity in the vicinity of the model location is about 0.01° upwash. When an upwash equal to the negative of that at the model location obtained from the first pass is used as the upstream value in the second pass (i.e., $v_{up} = -\Delta\alpha_1$) then the second pass WIAC assessments show zero or small positive upwash at the model. Without an independently measured flow angularity somewhere in the test section during the test, this second pass through WIAC cannot be any more meaningful than the first pass; a flow angle criterion must be satisfied somewhere in the test section in order to have properly aligned the flow and deduce an angle-of-attack correction. These calibration points, using the upright and inverted model data, give the "zero-lift" value for this upstream flow angularity; it should be measured during the tunnel run for each data point.

Typical NTF Pathfinder I Data

The NTF Pathfinder I data used here for assessment by the WIAC procedures had been reduced before the tunnel calibration had been included in the tunnel data-reduction process. Thus, the reference values of static pressure and corresponding values of Mach number and dynamic pressure were used to compute C_p, etc. in the data reduction. This is evident in Figure 12, where tunnel sidewall centerline C_p data are shown. It can be seen that the far upstream values of the C_p from the model wall-pressure signature, denoted by the solid symbols, do not vanish. In addition, these model signature C_p data show a scatter estimated to be about ± 0.003 which is larger than the indicated gauge accuracy and therefore due perhaps to local wall or pressure tap imperfections. When the calibration run ("tunnel-empty") wall-pressure signature at the same tunnel M and Re is

subtracted (as a tare) from the model wall-pressure signature, the data denoted by the open symbols (model-no model) are obtained. It can be seen in taking such a tare correction of the wall C_p data, that one must make a corresponding Mach number correction or accounting and also (perhaps) an unknown flow angularity correction.

The WIAC codes have been run with both tared and untared data in the outer boundary condition. The formulation of the PANCOR code was made assuming that one should not make such tare corrections since one is in effect subtracting out part of the tunnel interference present in the test data point. On the other hand, boundary conditions presently in the TUNCOR code seem to be more appropriate, particularly at the upstream and downstream ends of the test section, to properties exhibited by the tared wall-pressure signature. Details and conclusions relating to this matter are still being investigated in both WIAC codes. As has been seen, both codes give very good assessment of the tunnel calibration, where one must use the untared signature.

Sample PANCOR code results for ΔM are presented as a contour plot in the wing-plane on Figure 13. The data were taken at $M_T = 0.6$, $\alpha_T = 4.3^o$, and $Re_c = 2x10^6$ and the WIAC results are for no tare correction of the tunnel wall C_p signature. It can be seen that the principal part of the correction is that due to the tunnel calibration, -0.0037, as previously quoted in Table VII. The ΔM deviations from this value over the model are seen to be an order of magnitude smaller, tending to confirm the NTF slotted-wall test section design results given in Table VI.

Sample TUNCOR code results showing the influence of $\Delta\alpha$ on the lift curves at M = 0.6 and 0.8 for $Re_c = 2x10^6$ are given in Figure 14. The tunnel-wall C_p signature used in the WIAC boundary condition is that "tared" using the corresponding calibration wall signature. It can be seen that the angle-of-attack corrections are indeed small and positive for positive C_L. This also agrees with the NTF slotted-wall tunnel design estimates based on classical theory and given in Table VI. However, the small size of these corrections does not necessarily mean that they are of no concern or consequence. The sensitivity of the supercritical flow on the Pathfinder I wing to such small changes in the tunnel Mach number and angle of attack was demonstrated in reference 58.

CONCLUSIONS

Several general conclusions are drawn here for the WIAC applications to both 2-D and 3-D transonic wind-tunnel data. Recall that a number of specific findings (conclusions) for the 2-D nonlinear WIAC have already been given in the section of this paper concerning application to the 0.3-m TCT airfoil data.

General conclusions with respect to the 2-D airfoil-tunnel WIAC are:

(a) The nonlinear, 4-wall, posttest WIAC procedures offer a means for assessing and correcting transonic wind-tunnel data to accuracies approaching present-day requirements for airfoil test results.

(b) At transonic flow conditions with very large regions of supercritical flow, the complicated 3-D sidewall boundary-layer interaction is inadequately modelled by simple approximations; further work is required for this aspect.

General conclusions with respect to the 3-D configuration-tunnel WIAC are:

(a) A high degree of quality is needed in the wall C_p signature data since the signal (to noise) is small relative to that from 2-D airfoil tunnels.

(b) For one measured-data, C_p, array WIAC procedures, some flow angle data, taken during the model test runs, is also required.

(c) The nonlinear 3-D WIAC is just now being applied to real 3-D transonic data while the transonic limits of applicability of the linear 3-D WIAC are still being investigated; initial results from both procedures are encouraging.

REFERENCES

1. Prandtl, L.: Tragflügeltheorie, Part II. Nachrichten der K. Gesellschaft der Wissenschaften zu Göttingen, 1919.

2. Prandtl, L.; and Tietjens, O. G.: Applied Hydro- and Aerodynamics, Dover, NY, 1957.

3. Prandtl, L.: Tragflügeltheorie II. Ludwig Prandtl gesammelte Abhandlunge, Springer-Verlag, 1961, pp. 346-372.

4. Wright, Ray H.; and Ward, Vernon G.: NACA Transonic Wind-Tunnel Test Sections. NACA Report 1231, 1955.

5. Becker, John W.: The High-Speed Frontier - Case Histories of Four NACA Programs, 1920-1950. NASA SP-445, 1980, pp. 61-118.

6. Hansen, James R.: Engineer in Charge: A History of the Langley Aeronautical Laboratory, 1917-1958. NASA SP-4305, 1987, pp. 311-331.

7. Theodorsen, T.: The Theory of Wind-Tunnel Wall Interference. NACA Report No. 410, 1931.

8. Allen, H. Julian; and Vincenti, Walter G.: Wall Interference in a Two-Dimensional-Flow Wind Tunnel, With Consideration of the Effect of Compressibility. NACA Report No. 782, 1944.

9. Goethert, B. H.: Transonic Wind Tunnel Testing. Edited by W. C. Nelson. AGARDograph 49. Pergamon Press, 1961.

10. Pope, Alan; and Harper, John J.: Low-Speed Wind Tunnel Testing. John Wiley & Sons, Inc., 1966, Chapter 6, Wind Tunnel Boundary Conditions.

11. Pankhurst, R. C.; and Holder, D. W.: Wind-Tunnel Technique, An Account of Experimental Methods in Low- and High-Speed Wind Tunnels. Sir Isaac Pitman & Sons, LTD., 1952 (reprinted with corrections 1965), Chapter 8, Tunnel Interference Effects.

12. Garner, H. C.; Rogers, E. W. E.; Acum, W. E. A.; and Maskell, E. C.: Subsonic Wind Tunnel Wall Corrections. AGARDograph 109, 1966.

13. Pindzola, M.; and Lo, C. F.: Boundary Interference at Subsonic Speeds in Wind Tunnels with Ventilated Walls. AEDC TR-69-47, 1969.

14. Keller, J. D.; and Wright, R. H.: A Numerical Method of Calculating the Boundary-Induced Interferences in Slotted or Perforated Wind Tunnels of Rectangular Cross Section. NASA TR R-379, 1971.

15. Keller, J. D.: Numerical Calculation of Boundary-Induced Interference in Slotted or Perforated Wind Tunnels Including Viscous Effects in Slots. NASA TN D-6871, 1971.

16. Murman, Earll M.; and Cole, Julian D.: Calculation of Plane Steady Transonic Flows. AIAA J., vol. 9, Jan. 1971, pp. 114-121.

17. Murman, Earll M.: Computation of Wall Effects in Ventilated Transonic Wind Tunnels. AIAA Paper 72-1007, 1972.

18. Jacocks, J. L.: An Investigation of the Aerodynamic Characteristics of Ventilated Test Section Walls for Transonic Wind Tunnels. Ph.D. Dissertation, University of Tennessee, December 1976. (Also available as AEDC-TR-77-61, 1977.)

19. Kraft, E. M.; Ritter, A.; and Laster, M. L.: Advances at AEDC in Treating Transonic Wind Tunnel Wall Interference. 15th Congress, International Council of the Aeronautical Sciences, London, U.K., Sept. 7-12, 1986. Proceedings, Vol. 2, 1986, pp. 748-769. (ICAS-86-1.6.1).

20. Everhart, Joel L.: Theoretical and Experimental Studies of the Transonic Flow Field and Associated Boundary Conditions Near a Longitudinally-Slotted Wind-Tunnel Wall. D.Sc. Dissertation, George Washington University, Feb., 1988.

21. Ferri, A.; and Baronti, P.: A Method for Transonic Wind-Tunnel Corrections. AIAA J., vol. 11, Jan. 1973, pp. 63-66.

22. Sears, W. R.: Self Correcting Wind Tunnels. The Aeronautical Journal, vol. 78, Feb./Mar. 1974, pp. 80-89.

23. Kemp, William B., Jr.: Toward the Correctable-Interference Transonic Wind Tunnel. AIAA Ninth Aerodynamic Testing Conference, June 1976, pp. 31-38.

24. Kemp, W. B.: Transonic Assessment of Two-Dimensional Wind Tunnel Wall Interference Using Measured Wall Pressures. NASA CP-2045, 1978, pp. 473-486.

25. AGARD: Wind Tunnel Design and Testing Techniques. Proceedings of the Fluid Dynamics Panel Symposium, London, Oct. 6-8, 1975, AGARD-CP-174, 1976.

26. Elsenaar, A. (Editor): Two-Dimensional Transonic Testing Methods, Final Report. NLR-TR-83086, GARTEUR/TP-011 (work completed July 1981).

27. AGARD: Windtunnel Capability Related to Test Sections, Cryogenics, and Computer-Windtunnel Integration. Report of The Windtunnel Testing Techniques Sub-Committee of the AGARD Fluid Dynamics Panel, AGARD-AR-174, 1982.

28. AGARD: Wall Interference in Wind Tunnels. 50th Fluid Dynamics Panel Specialists' Meeting, London, England, May 19-20, 1982, AGARD-CP-335.

29. Newman, P. A.; and Barnwell, R. W., editors: Wind Tunnel Wall Interference Assessment/Correction, 1983. A workshop held at NASA Langley Research Center, Hampton, VA., Jan. 25-26, 1983. NASA CP-2319, 1984.

30. AGARD: Wind Tunnel & Testing Techniques. Symposium, Cesme, Turkey, Sept. 26-29, 1983, AGARD-CP-348.

31. Mokry, M.; Chan, Y. Y.; and Jones, D. J.; Edited by Ohman, L. H.: Two-Dimensional Wind Tunnel Wall Interference. AGARD AG-281, 1983.

32. Hornung, H.; and Stanewsky, E. (editors): Adaptive Wall Wind Tunnels and Wall Interference Correction Methods. Oct. 15-17, 1984, Rep. no. DFVLR-IB-222-84-A-37, 1984.

33. Newman, P. A.; Mineck, R. E.; Barnwell, R. W.; and Kemp, W. B., Jr.: Wind Tunnel Wall Interference. Langley Symposium on Aerodynamics, Vol. I, NASA CP-2397, 1986, pp. 225-260.

34. AGARD: Aerodynamic Data Accuracy and Quality: Requirements and Capabilities in Wind Tunnel Testing. AGARD Fluid Dynamics Panel Symposium, Naples, Italy, Sept. 28 - Oct. 1, 1987. (AGARD CP-429, 1988.)

35. Tuttle, M. H.; and Cole, K. L.: Wind Tunnel Wall Interference (Jan. 1980 - May 1988) - A Selected, Annotated Bibliography. NASA TM-4061, 1988.

36. Kemp, W. B., Jr.: TWINTAN: A Program for Transonic Wall Interference Assessment in Two-Dimensional Wind Tunnels. NASA TM-81819, 1980.

37. Kemp, W. B., Jr.; and Adcock, J. B.: Combined Four-Wall Interference Assessment in Two-Dimensional Airfoil Tests. AIAA Paper 82-0586, 1982. (AIAA J., Vol. 21, 1983, pp. 1353-1359).

38. Gumbert, C. R.; Newman, P. A.; Kemp, W. B., Jr.; and Adcock, J. B.: Adaptation of a Four-Wall Interference Assessment/Correction Procedure for Airfoil Tests in the 0.3-m TCT, pp. 393-414 of reference 29.

39. Kemp, W. B., Jr.: TWINTN4: A Program for Transonic Four-Wall Interference Assessment in Two-Dimensional Wind Tunnels. NASA CR-3777, 1984.

40. Gumbert, C. R.; and Newman, P. A.: Validation of a Wall Interference Assessment/Correction Procedure for Airfoil Tests in the Langley 0.3-m Transonic Cryogenic Tunnel. AIAA Paper 84-2151, 1984.

41. Gumbert, C. R.: User Manual for 0.3-m TCT Wall-Interference Assessment/Correction Procedure: 8- by 24-Inch Airfoil Test Section. NASA TM-87582, 1985.

42. Green, L. L.; and Newman, P. A.: Transonic Wall Interference Assessment and Corrections for Airfoil Data from the 0.3-m TCT Adaptive Wall Test Section. AIAA Paper 87-1431, 1987.

43. Green, L. L. R.: Wall Interference Assessment and Corrections for Transonic Adaptive Wall Airfoil Data. M.S. Thesis, George Washington University, April 1988.

44. Gumbert, C. R.: Wall Interference Assessment/Correction of Data from Tests of a CAST 10-2/DOA 2 Airfoil in the Langley 0.3-m Transonic Cryogenic Tunnel. M.S. Thesis, George Washington University, May 1988.

45. Rizk, M. H.; Hafez, M.; Murman, E. M.; and Lovell, D.: Transonic Wind Tunnel Wall Interference Corrections for Three-Dimensional Models. AIAA Paper 82-0588, 1982.

46. Rizk, M. H.; and Murman, E. M.: Wind Tunnel Wall Interference Corrections for Aircraft Models in the Transonic Regime. J. of Aircraft, Vol. 21, Jan. 1984, pp. 54-61.

47. Rizk, M. H.; Smithmeyer, M. G.; and Murman, E. M.: Wind Tunnel Wall Interference Corrections for Aircraft Models, pp. 301-322 of reference 29.

48. Rizk, M. H.: Improvements in Code TUNCOR for Calculating Wall Interference Corrections in the Transonic Regime. AEDC-TR-86-6, 1986.

49. Kemp, W. B., Jr.: A Slotted Test Section Numerical Model for Interference Assessment. J. of Aircraft, Vol. 22, Mar. 1985, pp. 216-222.

50. Kemp, W. B., Jr.: Computer Simulation of a Wind Tunnel Test Section with Discrete Finite-Length Wall Slots. NASA CR-3948, 1986.

51. Kemp, W. B., Jr.: A Panel Method Procedure for Interference Assessment in Slotted-Wall Wind Tunnels. AIAA Paper 88-2537, 1988.

52. Rizk, M. H.; and Lovell, D. R.: Two-Dimensional Transonic Wind Tunnel Wall Interference Corrections Based on the Euler Equations. AIAA Paper 86-0124, 1986.

53. Rizk, M. H.; Lovell, D. R.; and Baker, T. J.: A Procedure Based on the Euler Equations for Correcting Transonic Wind Tunnel Wall Interference. AIAA Paper 88-0141, 1988.

54. Murman, E. M.: A Correction Method for Transonic Wind Tunnel Wall Interference. AIAA Paper 79-1533, 1979.

55. Zhang, Q.: Two-Dimensional Subsonic and Transonic Wind Tunnel Wall Interference Corrections for Varied Walls. Acta Aerodynamic Sinica, Vol. 5, June 1987, pp. 132-140 (in Chinese).

56. Lo, C. F.; and Sickles, W. L.: Two-Measured Variable Method for Wall Interference Assessment/Correction. Transonic Symposium, NASA CP-3020, vol. I, 1989, pp. 853-866.

57. Stahara, S. S.; and Spreiter, J. R.: A Transonic Wind Tunnel Interference Assessment: Axisymmetric Flows. AIAA J., Vol. 18, Jan. 1980, pp. 63-71.

58. McKinney, L. W.; Bruce, W. E., Jr.; and Gloss, B. B.: National Transonic Facility Status. Transonic Symposium, NASA CP-3020, 1989. (Paper 1, vol. II.)

59. Kilgore, R. A.; Dress, D.A.; Wolf, S. W. D.; and Britcher, C. P.: Test Techniques - A Survey Paper on Cryogenic Tunnels, Adaptive Wall Test Sections, and Magnetic Suspension and Balance Systems. Transonic Symposium, NASA CP-3020, vol. I, 1989, pp. 705-741.

60. Kraft, E. M.: An Overview of Approaches and Issues for Wall Interference Assessment/Correction, pp. 3-20 of reference 29.

61. Schairer, E. T.: Two-Dimensional Wind Tunnel Interference from Measurements on Two Contours. J. of Aircraft, Vol. 21, June 1984, pp. 414-419.

62. Ashill, P. R.; and Weeks, D. J.: A Method for Determining Wall-Interference Corrections in Solid-Wall Tunnels from Measurements of Static Pressure at the Walls. Paper No. 1 in reference 28.

63. Kraft, E. M.; and Dahm, W. J. A.: Direct Assessment of Wall Interference in a Two-Dimensional Subsonic Wind Tunnel. AIAA Paper 82-0187, 1982.

64. Capelier, C.; Chevallier, J. P.; and Bouniol, F.: Nouvelle Methode de Correction des Effets de Parois en Courant Plan. La Recherche Aerospatiale, Jan./Feb. 1978, pp. 1-11.

65. Sawada, H.: A General Correction Method of the Interference in Two-Dimensional Wind Tunnels with Ventilated Walls. Transactions of the Japan Society for Aeronautical and Space Sciences, Vol. 21, Aug. 1978, pp. 57-68.

66. Mokry, M.; and Ohman, L. H.: Application of the Fast Fourier Transform to Two-Dimensional Wind-Tunnel Wall Interference. J. of Aircraft, Vol. 17, June 1980, pp. 402-408.

67. Smith, J.: A Method for Determining 2D Wall Interference on an Aerofoil from Measured Pressure Distributions near the Walls and on the Model. NLR TR 81016 U, 1981.

68. Rizk, M. H.; and Smithmeyer, M. G.: Wind Tunnel Wall Interference Corrections for Three-Dimensional Flows. J. of Aircraft, Vol. 19, June 1982, pp. 465-472.

69. Mokry, M.: Subsonic Wall Interference Corrections for Half-Model Tests Using Sparse Wall Pressure Data. Euromech Colloquium No. 187, Gottingen, FRG, Oct. 15-17, 1984. Report No. LR-616; NRC-25132, DCAF F002839, Nov. 1985.

70. Schulz, G.: A Universal 3-Dimensional Wall Pressure Correction Method for Closed Rectangular Subsonic Wind Tunnel Test Sections (Displacement, Downwash, Streamline Curvature). ESA-TT-800, June 1983, (translation of DFVLR-FB-82-19).

71. Labrujere, T. E.: Correction for Wall-Interference by Means of a Measured Boundary Condition Method. Rep. No. NLR-TR-84114-U, B8671294, ETN-86-98650, Nov. 21, 1984.

72. Moses, D. F.: Wind Tunnel Wall Corrections Deduced by Iterating From Measured Wall Static Pressure. AIAA J., Vol. 21, Dec. 1983, pp. 1667-1673.

73. Crites, R. A.: Transonic Wind Tunnel Boundary Interference - A Correction Procedure. AGARD Fluid Dynamics Panel Symposium on Aerodynamic Data Accuracy and Quality: Requirements and Capabilities in Wind Tunnel Testing, Naples, Italy, Sept. 28 - Oct. 1, 1987. Paper #15 of ref. 34.

74. Schairer, E. T.: Assessment of Lift- and Blockage-Induced Wall Interference in a Three-Dimensional Adaptive-Wall Wind Tunnel, pp. 89-100 of reference 29.

75. Barnwell, R. W.; and Sewall, W. G.: Similarity Rules for Effects of Sidewall Boundary Layer in Two-Dimensional Wind Tunnels. Paper No. 3 in reference 28.

76. Murthy, A. V.: Effect of Aspect Ratio on Sidewall Boundary-Layer Influences in Two-Dimensional Airfoil Testing. NASA CR-4008, 1986.

77. Ladson, C. L.; and Ray, E. J.: Evolution, Calibration, and Operational Characteristics of the Two-Dimensional Test Section of the Langley 0.3-Meter Transonic Cryogenic Tunnel. NASA TP-2749, 1987.

78. Ray, E. J.; and Ladson, C. L.: Review of the Advanced Technology Airfoil Test (ATAT) Program in the 0.3-m TCT, pp. 361-374 in reference 29.

79. Melnik, R. E.; Mead, N. R.; and Jameson, A.: A Multi-Grid Method for the Computation of Viscid/Inviscid Interaction on Airfoils, AIAA Paper 83-0234, 1983.

80. Swanson, R. C.; and Turkel, Eli: A Multistage Time-Stepping Scheme for the Navier-Stokes Equations. AIAA Paper 85-0035, 1985.

81. Ladson, C. L.; Hill, A. S.; and Johnson, W. G., Jr.: Pressure Distributions from High Reynolds Number Transonic Tests of an NACA 0012 Airfoil in the Langley 0.3-Meter Transonic Cryogenic Tunnel. NASA TM 100526, 1987.

82. Ladson, C. L.; and Hill, A. S.: High Reynolds Number Transonic Tests of an NACA 0012 Airfoil in the Langley 0.3-Meter Transonic Cryogenic Tunnel. NASA TM 100527, 1987.

83. Dress, D. A.; Johnson, C. B.; McGuire, P. D.; Stanewsky, E.; and Ray, E. J.: High Reynolds Number Tests of the CAST 10-2/DOA 2 Airfoil in the Langley 0.3-Meter Transonic Cryogenic Tunnel - Phase I. NASA TM-84620, 1983.

84. Dress, D. A.; Stanewsky, E.; McGuire, P. D.; and Ray, E. J.: High Reynolds Number Tests of the CAST 10-2/DOA 2 Airfoil in the Langley 0.3-Meter Transonic Cryogenic Tunnel - Phase II. NASA TM-86273, 1984.

85. Rebstock, R; and Lee, E. E., Jr.: Capabilities of Wind Tunnels with Two Adaptive Walls to Minimize Boundary Interference in 3-D Model Testing. Transonic Symposium, NASA CP- , 19 . (Paper of this compilation.)

86. Barnwell, R. W.: Design and Performance Evaluation of Slotted Walls for Two-Dimensional Wind Tunnels. NASA TM-78648, 1978.

Table I. Approaches to Establishing Corrected Transonic Wind Tunnel Test Conditions

CONVENTIONAL TUNNEL	
Test Data Point:	M_{ref}, α_{ref}
Mach Number Calibration:	$\Delta M_o \rightarrow M_T = M_{ref} + \Delta M_o$
Flow Angle Survey OR Model Upright/Inverted:	$\Delta\alpha_o \rightarrow \alpha_T = \alpha_{ref} + \Delta\alpha_o$
Wall Interference: (model/wall interaction)	$\Delta M_{WI} \rightarrow M_c = M_T + \Delta M_{WI}$ $\Delta\alpha_{WI} \rightarrow \alpha_c = \alpha_T + \Delta\alpha_{WI}$
WIAC	
Tunnel Interference:	$\Delta M_{WIAC} \rightarrow M_c = M_? + \Delta M_{WIAC}$ $\Delta\alpha_{WIAC} \rightarrow \alpha_c = \alpha_? + \Delta\alpha_{WIAC}$

Table II. Transonic Testing Factors Affecting WIAC for 2-D Airfoil Tunnel

MEASURED MODEL DATA

- 1-D C_p arrays with good resolution
- Drag rake for C_d

MEASURED FIELD DATA

- 1-D C_p arrays with good resolution and signal
- 1-D θ arrays are difficult to measure
- One θ required with C_p array

MODEL SUPPORT EFFECT

- Two SWBL interactions
- Flow may not be 2-D

TEST SECTION DESIGN

- Ventilated, generally near minimum blockage
- Adaptive

Table III. Relative Sizes of 0.3-m TCT Test Sections and Airfoil Models Used for Sample 2-D Results

Airfoil Section	chord length	thickness to chord τ	test section		half-height to chord (h/c)	model AR (2b/c)	Data ref.	WIAC ref.
			size	type				
NACA 0012	6"	.12	8"x 24"	SW	2.0	1.33	81, 82	40
	6.5"	.12	13"x 13"	AW	1.0	2.00		42, 43
	13"	.12	13"x 13"	AW	0.5	1.00		42, 43
CAST 10-2/DOA 2	3"	.121	8"x 24"	SW	4.0	2.67	84	40, 44
	6"	.121	8"x 24"	SW	2.0	1.33	83	40, 44

Table IV. Transonic Testing Factors Affecting WIAC for 3-D Configuration Tunnel

MEASURED MODEL DATA

- 2-D C_p arrays with sparse resolution OR none
- Force balances

MEASURED FIELD DATA

- 2-D C_p arrays w/ sparse resolution and small signal
- 2-D θ arrays are very difficult to measure
- Several θ's required with C_p array

MODEL SUPPORT EFFECT

- One SWBL interaction for semi-span models
- Sting/sector interference

TEST SECTION DESIGN

- Ventilated, criterion varies
- Pilot adaptive

Table V. Description of 3-D WIAC Codes

CODE CHARACTERISTICS	PANCOR	TUNCOR	EUCOR3D
Tunnel Type	Rectangular, slotted	Rectangular or circular	Rectangular
Flow Equation	Prandtl-Glauert	TSDE	Euler
Computational Mesh	Paneled Boundaries	Cartesian or cylindrical	H-H Body-fitted
Solution Method	Gaussian elimination	VLOR	Multi-grid, time stepping
Test Model	Distributed singularities based on C_L, C_D, C_M & approx. WBT shape	Small dist. shape BC for WBT α_w, α_t to match C_L, C_M	Exact shape BC for WBT α_w to match C_L 2-D strip boundary layer
Test Section Boundary singularities	Panels for solid walls, slats, reentry region, end planes & unperturbed outer flow Line sources for discrete slots	— —	— —
Boundary data	Wall shape, slot Kutta condition, Measured C_p rows	Measured C_p interpolated to computational mesh	Measured C_p interpolated to computational mesh
Other components	Distributed singularities for sting and sting support based on shape	None	None
Status	Validating on real data	Validating on real data	Code delivered, being debugged
Developed by	W. B. Kemp	M. H. Rizk, et al	M. H. Rizk, et al

Table VI. Numerically Simulated Wall Corrections for the Pathfinder I Model in NTF-Size Ideal Tunnels; $M_T = 0.82$, $\alpha_T = 1.93^\circ$, $C_L = 0.452$

TUNNEL	CORRECTIONS	
	ΔM	Δα
open-jet	-0.00063	-0.12693
solid-wall	+0.00127	+0.20445
classical theory for NTF Slot design*	+0.00030	+0.00612
finite TS length	+0.00050	+0.00612

*NTF test section design criterion was zero lift interference with all four walls slotted. Currently, sidewall slots are closed.

Table VII. WIAC Results for Two NTF Calibration Data Points at Re = 4×10^6/ft.

CONDITIONS		TUNCOR		PANCOR		EXP.	
M_T	v_{up}	ΔM	Δα	ΔM	Δα	ΔM	Δα*
0.6	0	-0.0035	-0.1328	-0.0037	-0.0866	-0.0034	≈+0.01
	$-\Delta\alpha_1$	-0.0034	+0.0177	-0.0037	0		
0.8	0	-0.0038	-0.1117	-0.0042	-0.1016	-0.0038	≈+0.01
	$-\Delta\alpha_1$	-0.0039	+0.0153	-0.0042	0		

*obtained from model upright and inverted tests

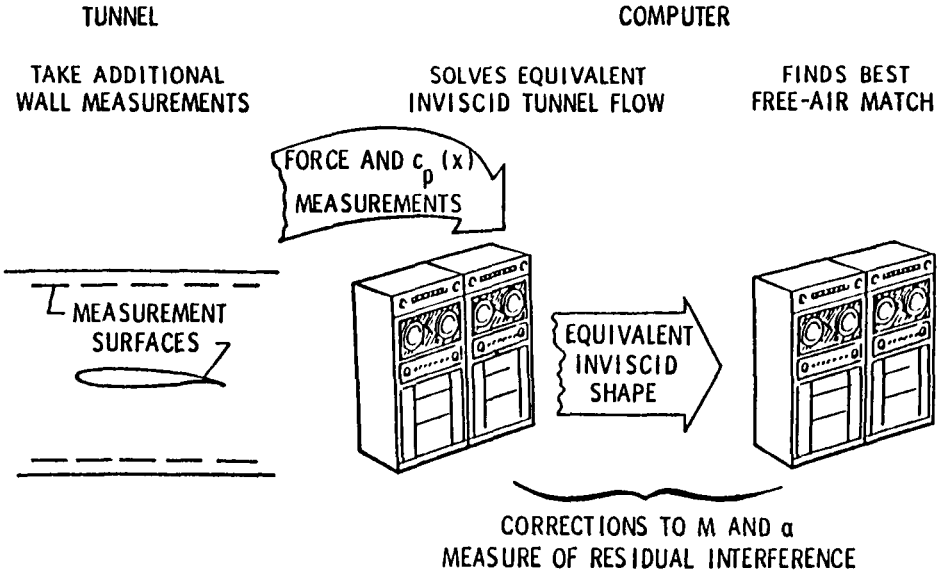

Figure 1. - Schematic of 2-D transonic WIAC concept.

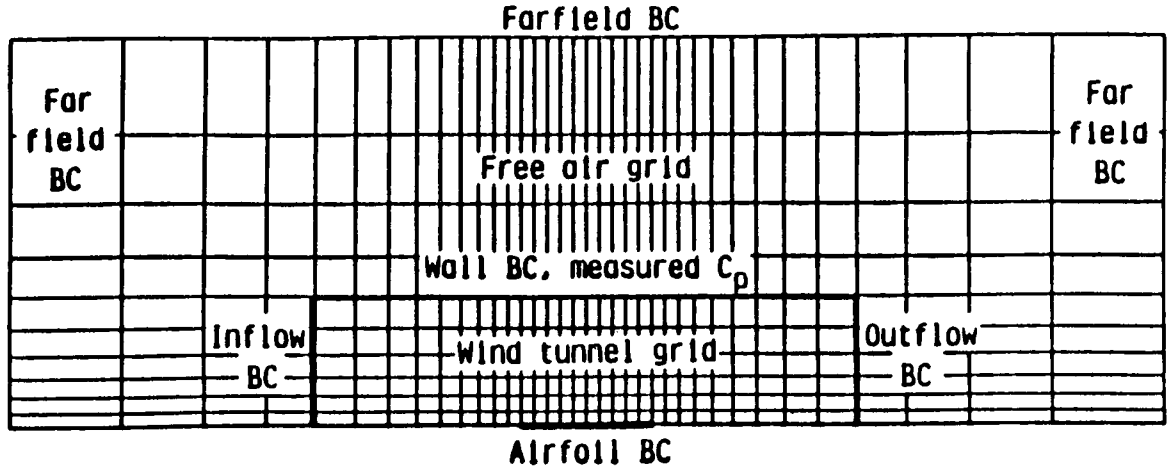

Figure 2. - Upper half-plane of Cartesian grid for 2-D TSDE WIAC code.

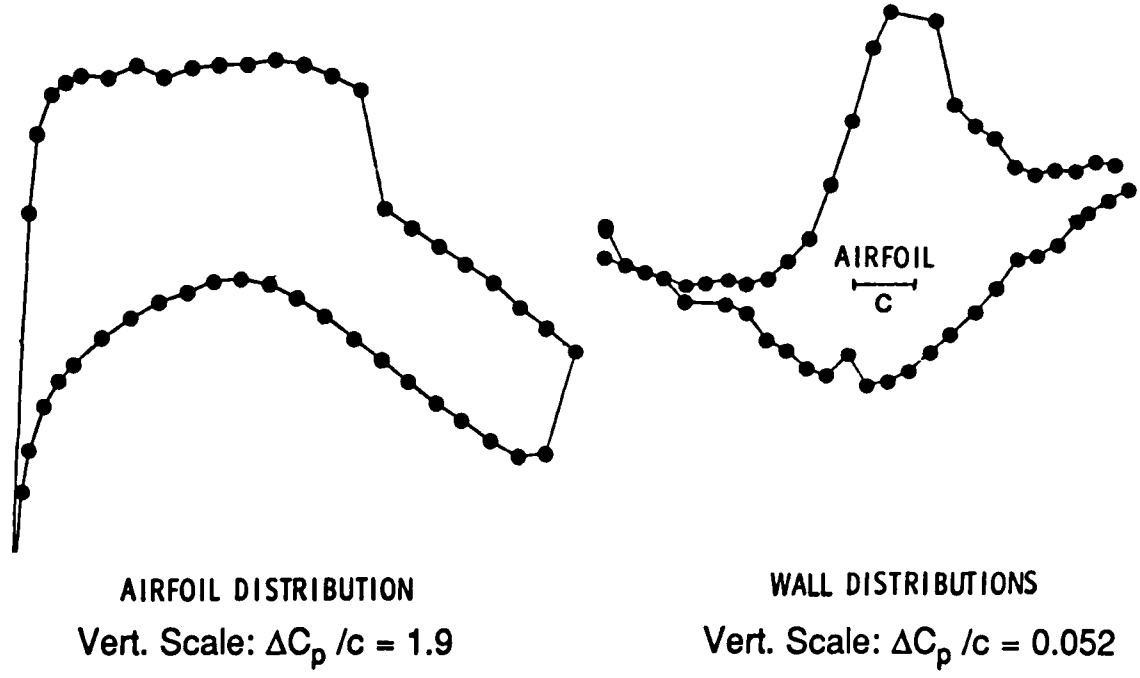

Figure 3. - Sample 0.3-m TCT slotted-wall and airfoil C_p distributions; $M_T = 0.765$, $\alpha_T = 2^\circ$, $c = 6"$, $Re_c = 6 \times 10^6$.

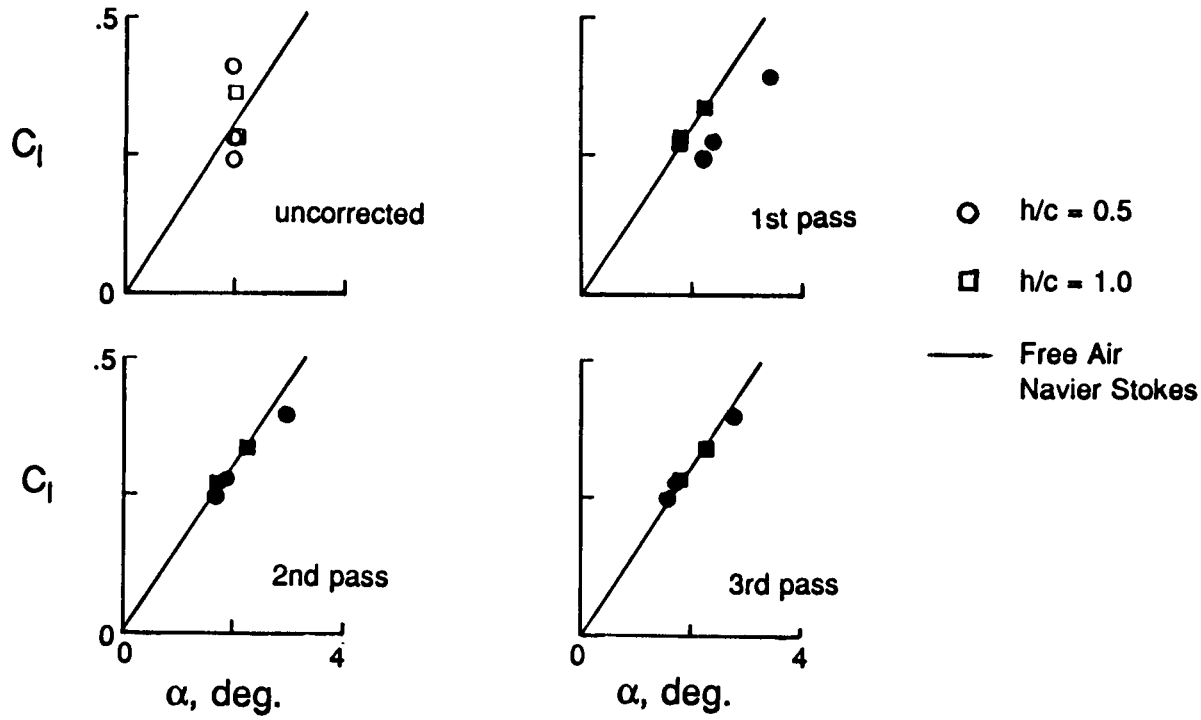

Figure 4. - Sample results for 2-D TSDE WIAC application to NACA 0012 airfoil data from the 0.3-m TCT with partially adapted walls; Lift curves at $M_T = 0.65$, $\alpha_T = 2^\circ$, $Re_c = 9 \times 10^6$.

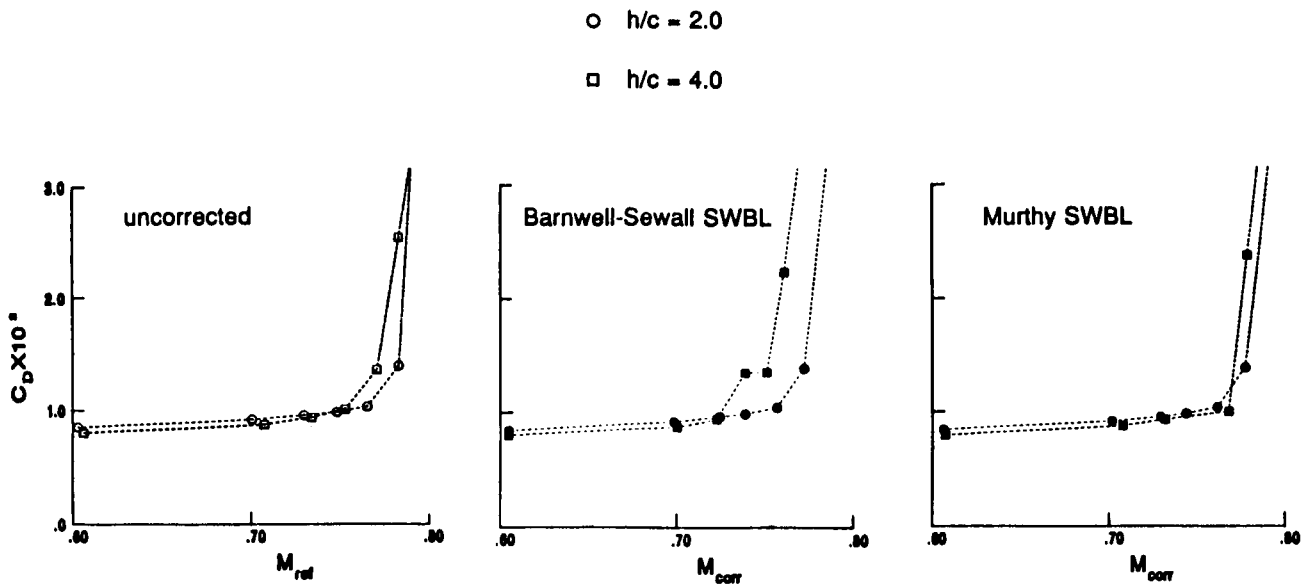

Figure 5. - Sample results for 2-D TSDE WIAC application to CAST 10-2/ DOA 2 airfoil data from the 0.3-m TCT with slotted walls; Drag-rise curves at $C_\ell = 0.5$, $Re_c = 15 \times 10^6$.

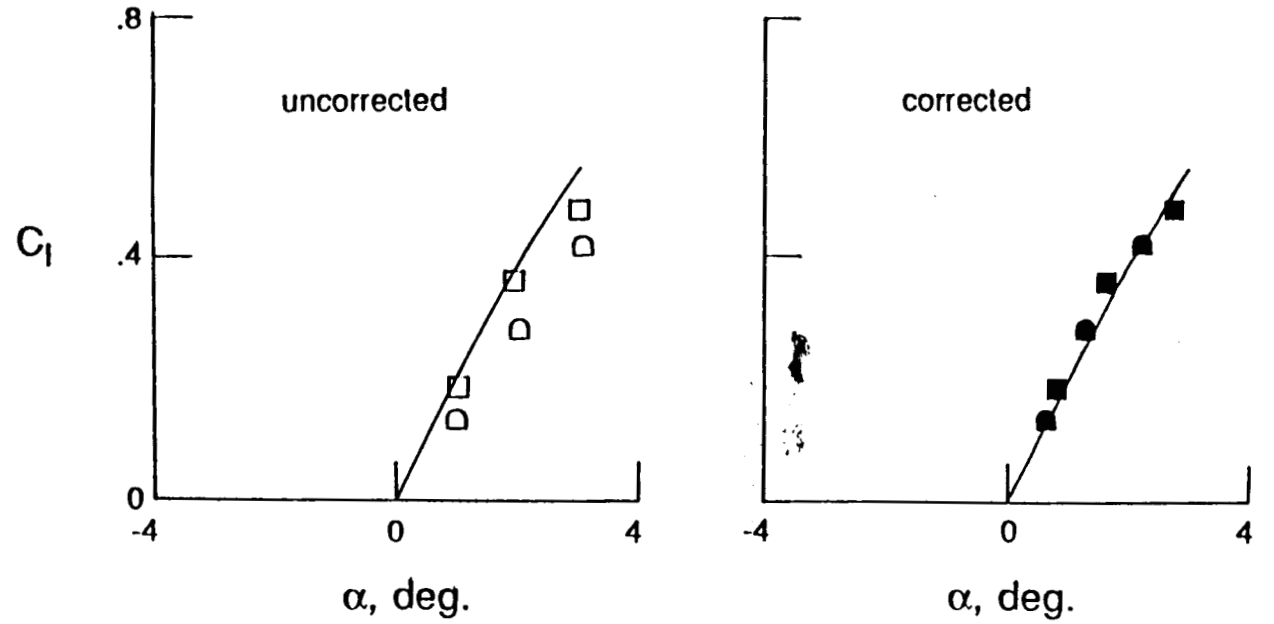

(a) Lift curves at $M_T = 0.76$.

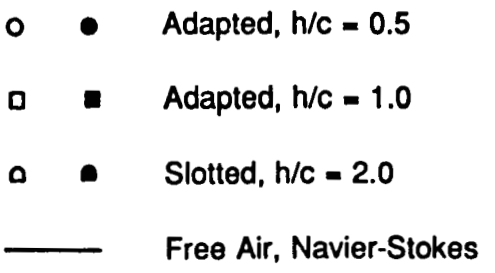

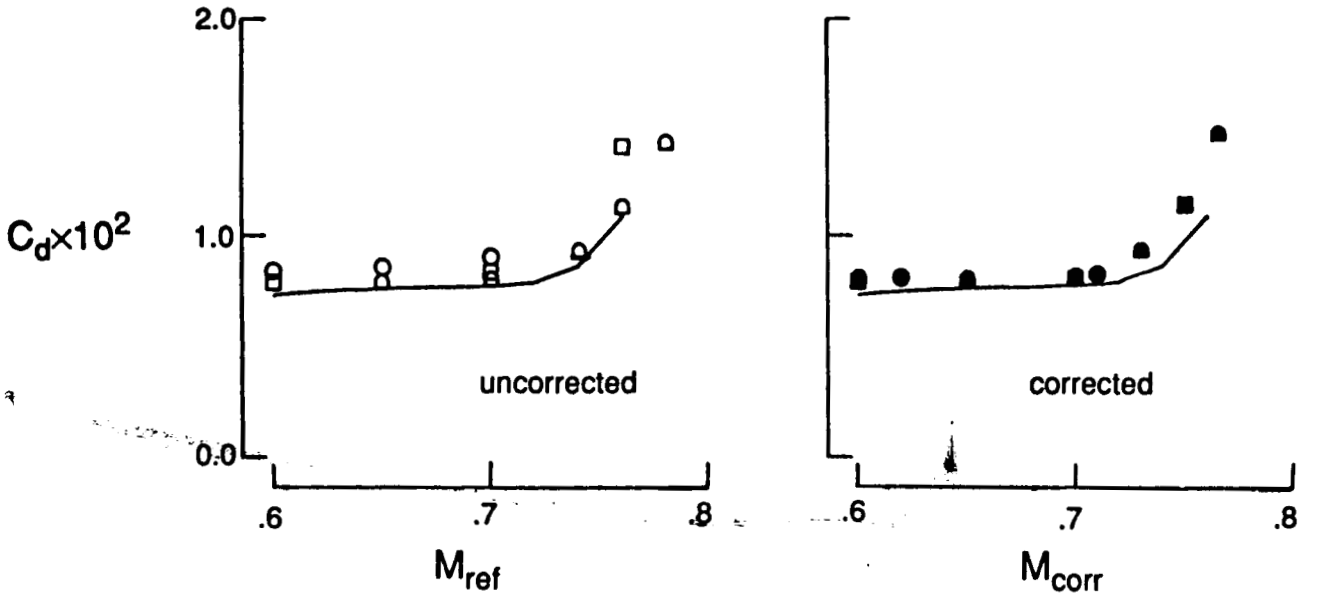

(b) Drag-rise curves at $C_\ell = 0.2$.

Figure 6. – Sample results for 2-D TSDE WIAC application to NACA 0012 airfoil data from the 0.3m TCT with slotted and fully-adapted walls at $Re_c = 9 \times 10^6$.

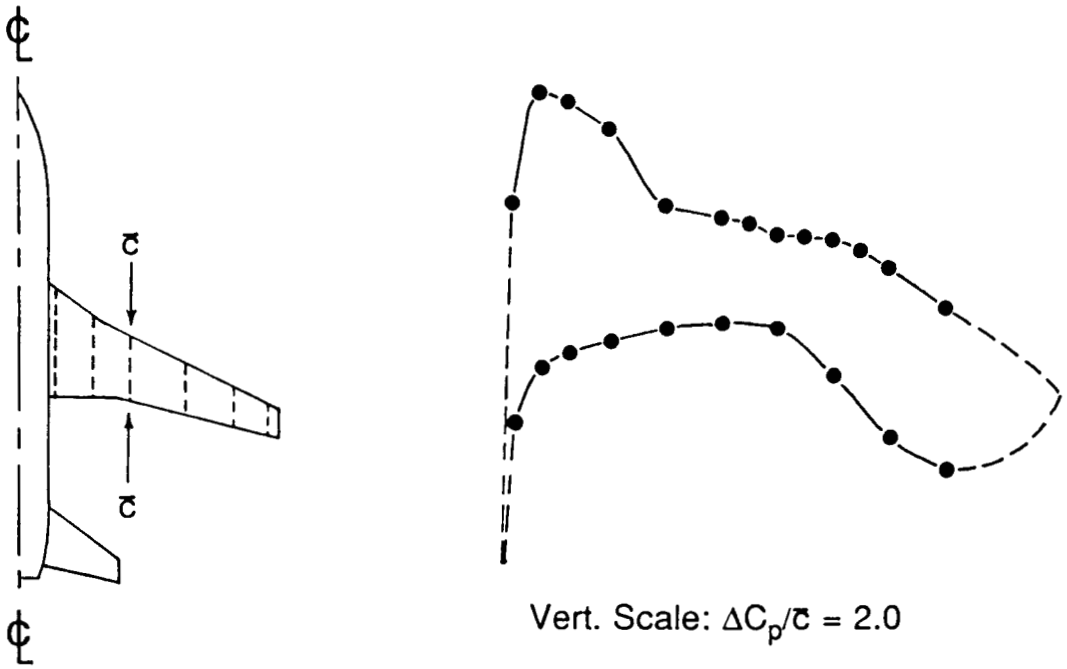

(a) Model wing C_p distribution

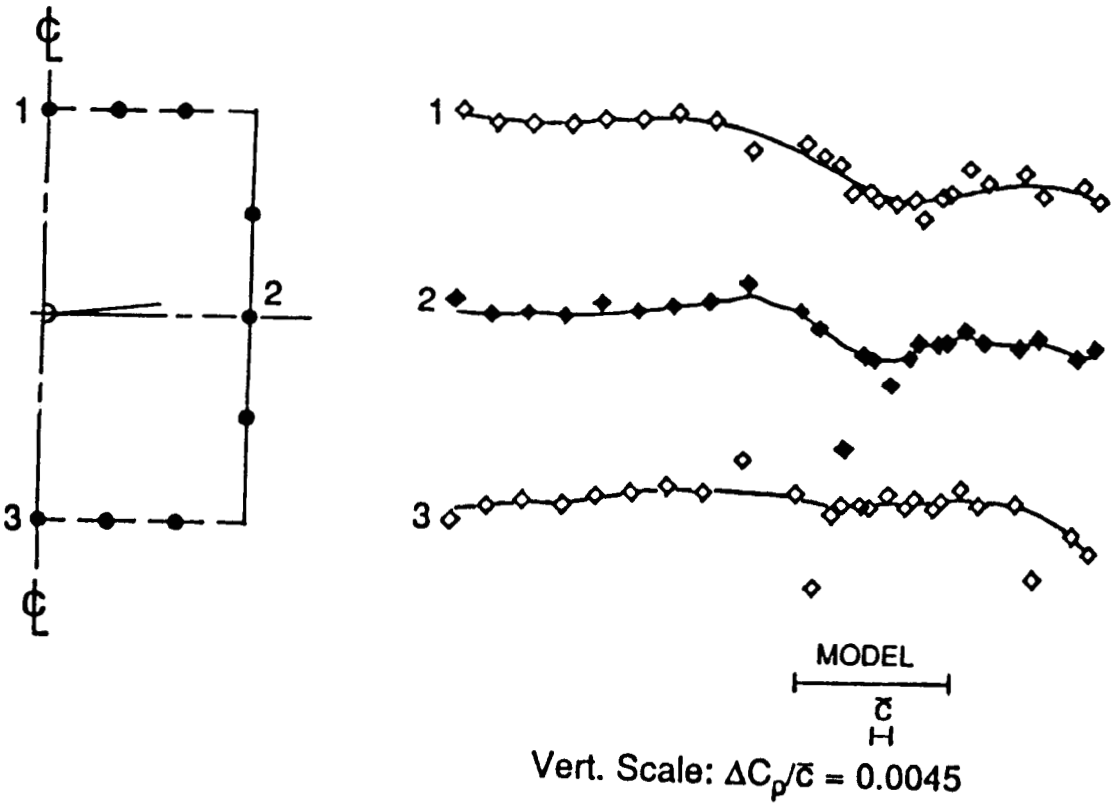

(b) Tunnel wall centerline C_p distributions

Figure 7. - Sample NTF slotted-wall and model C_p distributions; $M_T = 0.8$, $\alpha_T = 2.2^\circ$, $\bar{c} = 5.74"$, $b = 53.08"$, $Re_{\bar{c}} = 2 \times 10^6$.

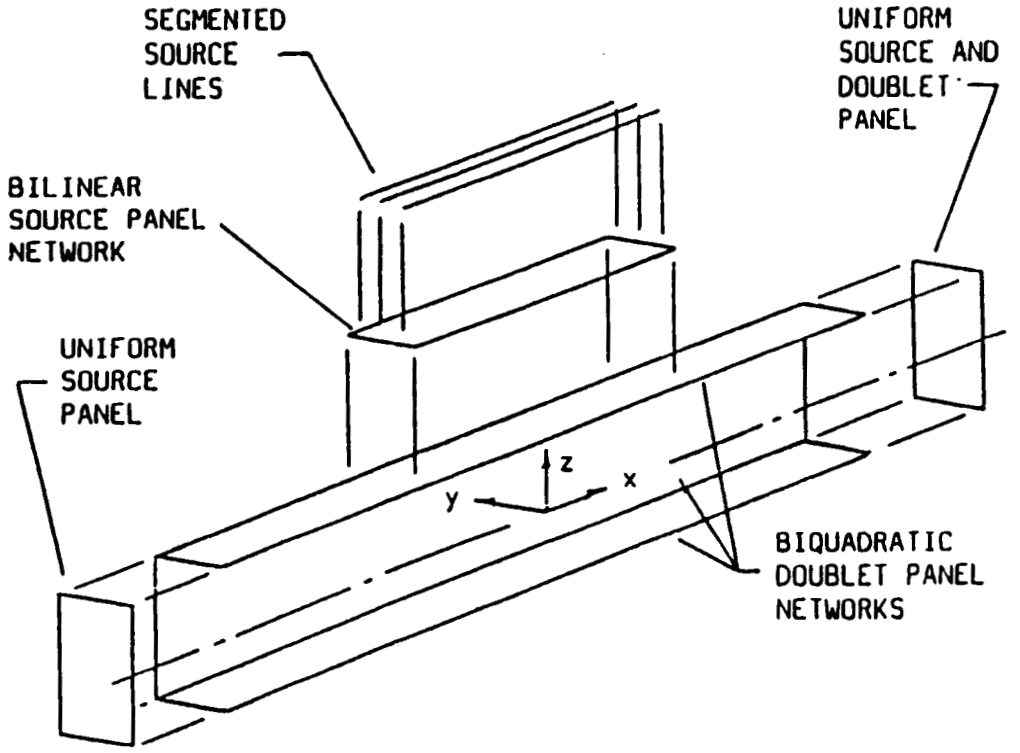

Figure 8. - Singularities representing the tunnel boundaries in the 3-D panel method WIAC code PANCOR.

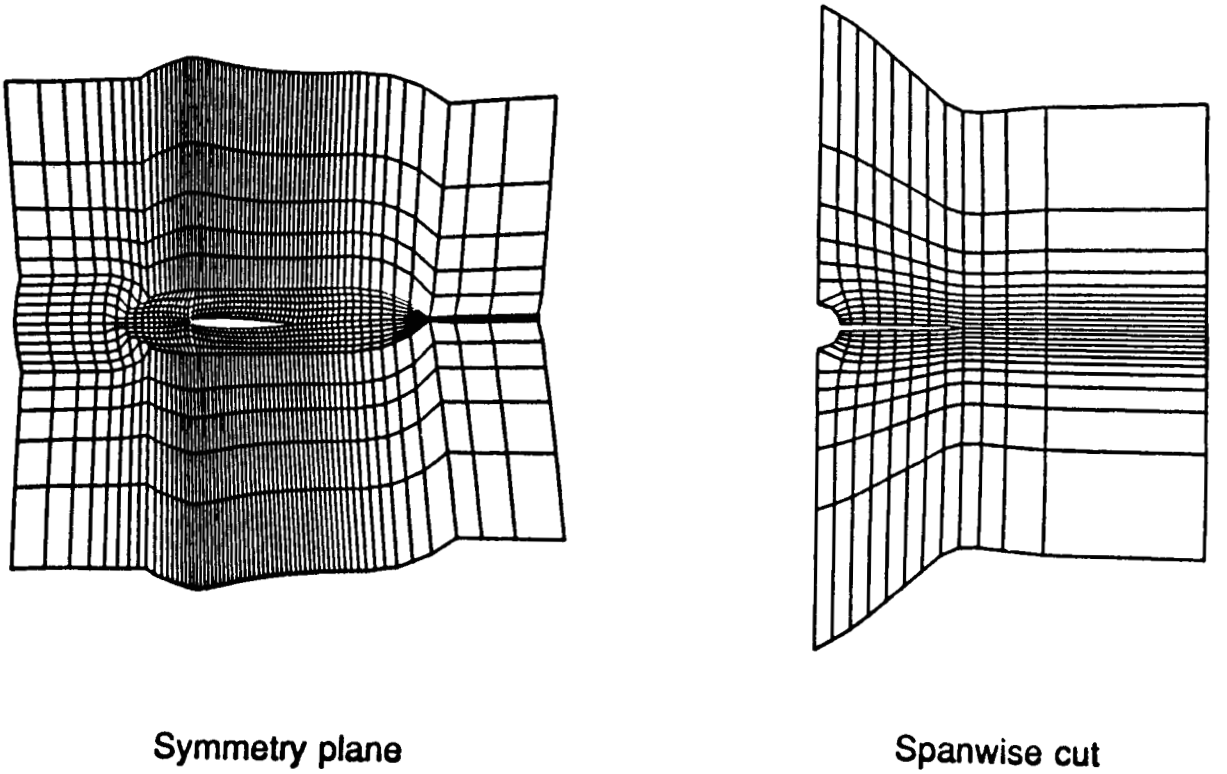

Figure 9. - Body-fitted H-H grid about wing-body configuration for the 3-D Euler equation WIAC code EUCOR3D.

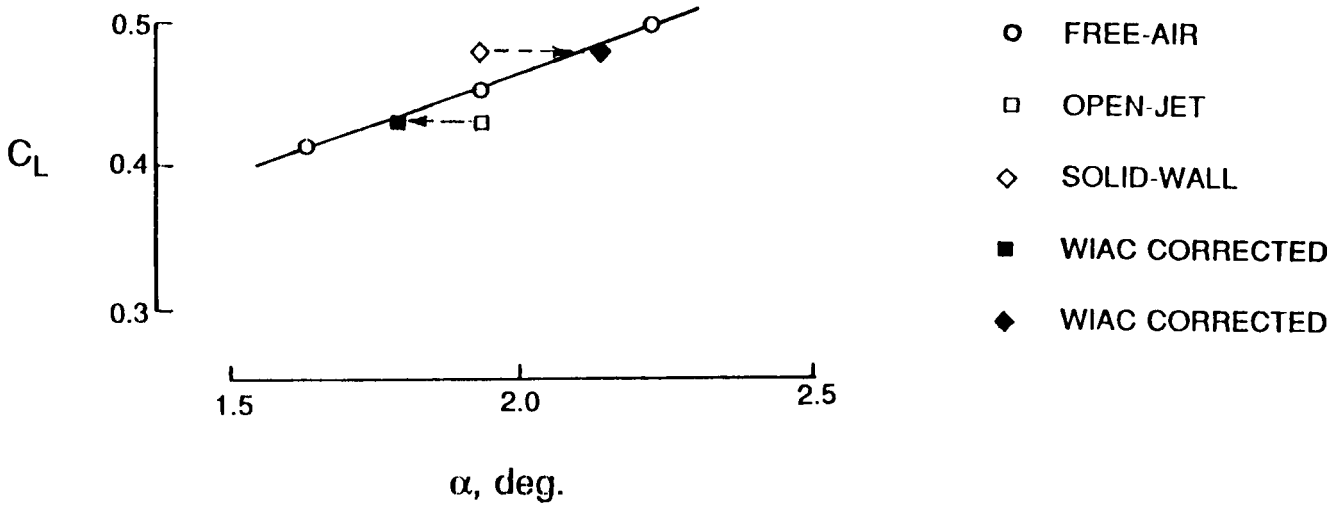

(a) Lift curve, C_L versus α.

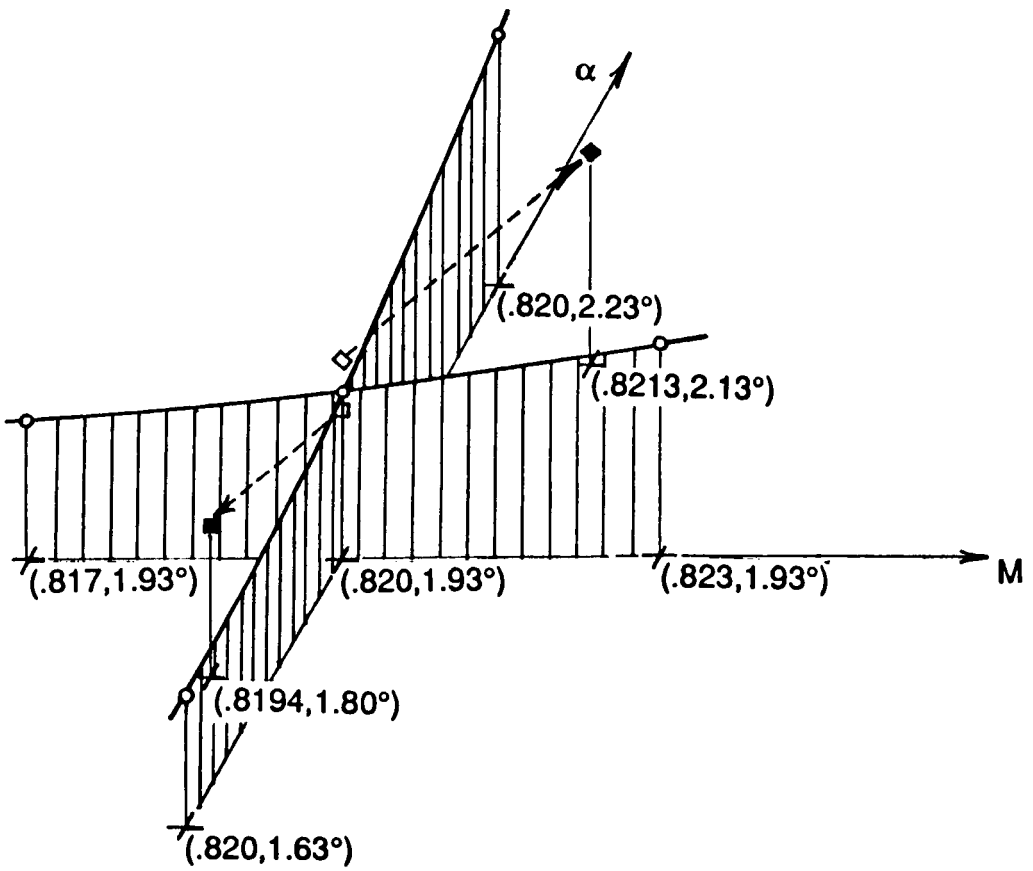

(b) Size of embedded supersonic flow region versus M and α.

Figure 10. - Numerically simulated wall corrections for the Pathfinder I model in NTF-size ideal tunnels; $M_T = 0.82$, $\alpha_T = 1.93^\circ$, $C_L = 0.452$.

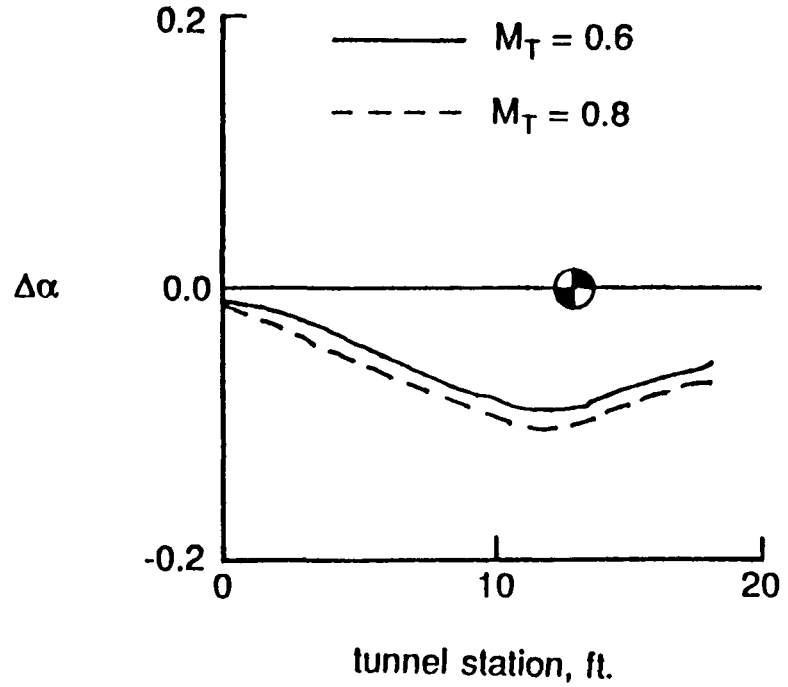

Figure 11. - Sample results for 3-D PANCOR WIAC application to calibration data from the NTF; Distribution of flow angularity along the tunnel centerline at Re = 4×10^6/ft.

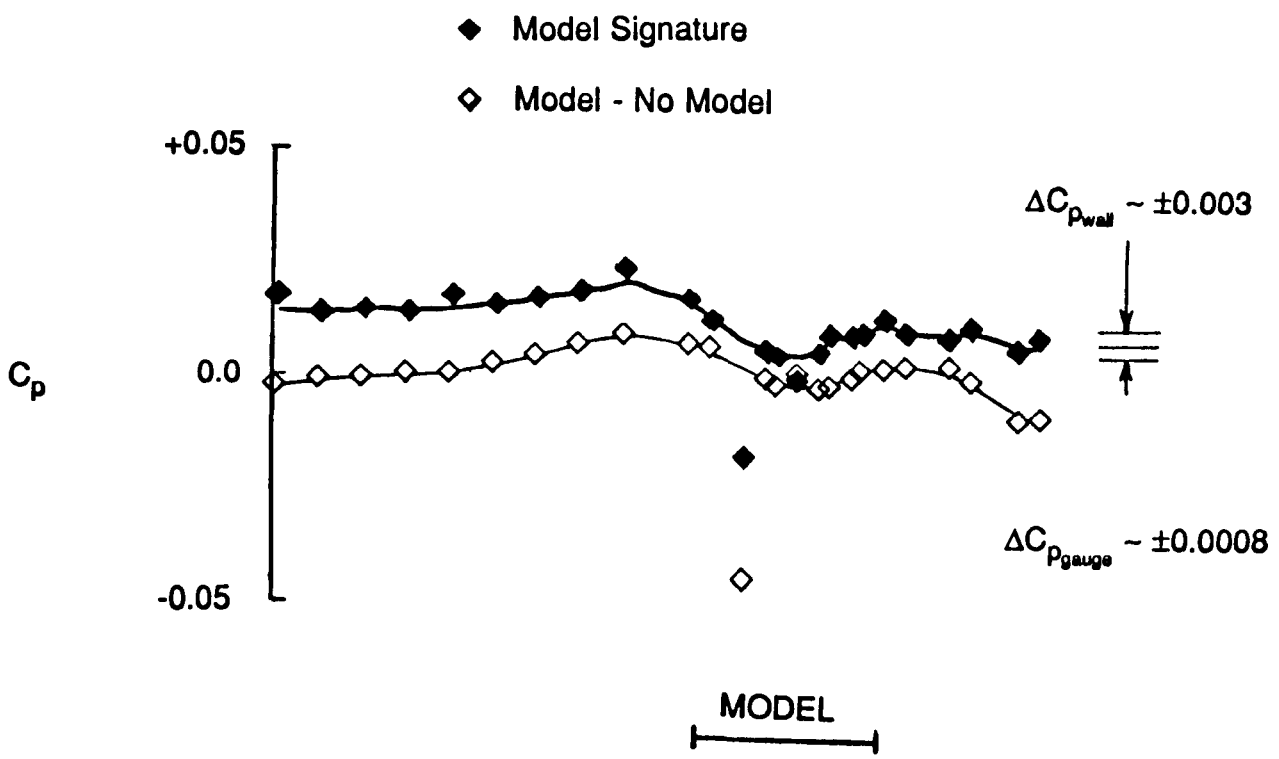

Figure 12. - Sample NTF sidewall centerline C_p distribution for the Pathfinder I model, with and without calibration data as tare; $M_T = 0.8$, $\alpha_T = 2.2^\circ$, $Re_c = 2 \times 10^6$.

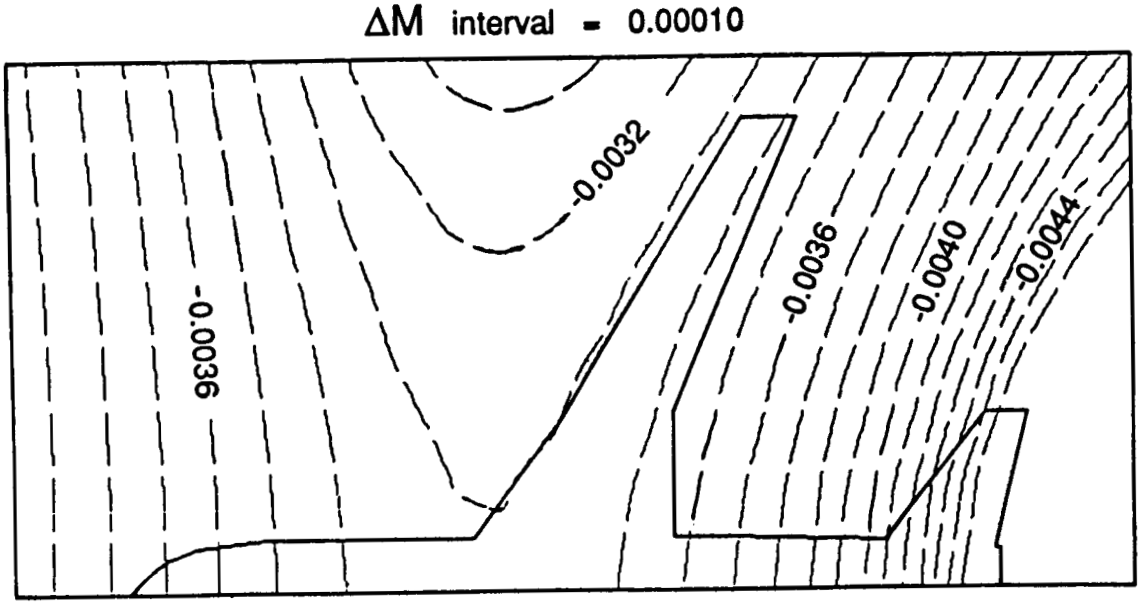

Figure 13. - Sample results for 3-D PANCOR WIAC application to Pathfinder I data from the NTF; Contour plot of ΔM at $M_T = 0.6$, $\alpha_T = 4.3^\circ$, $Re_c = 2 \times 10^6$.

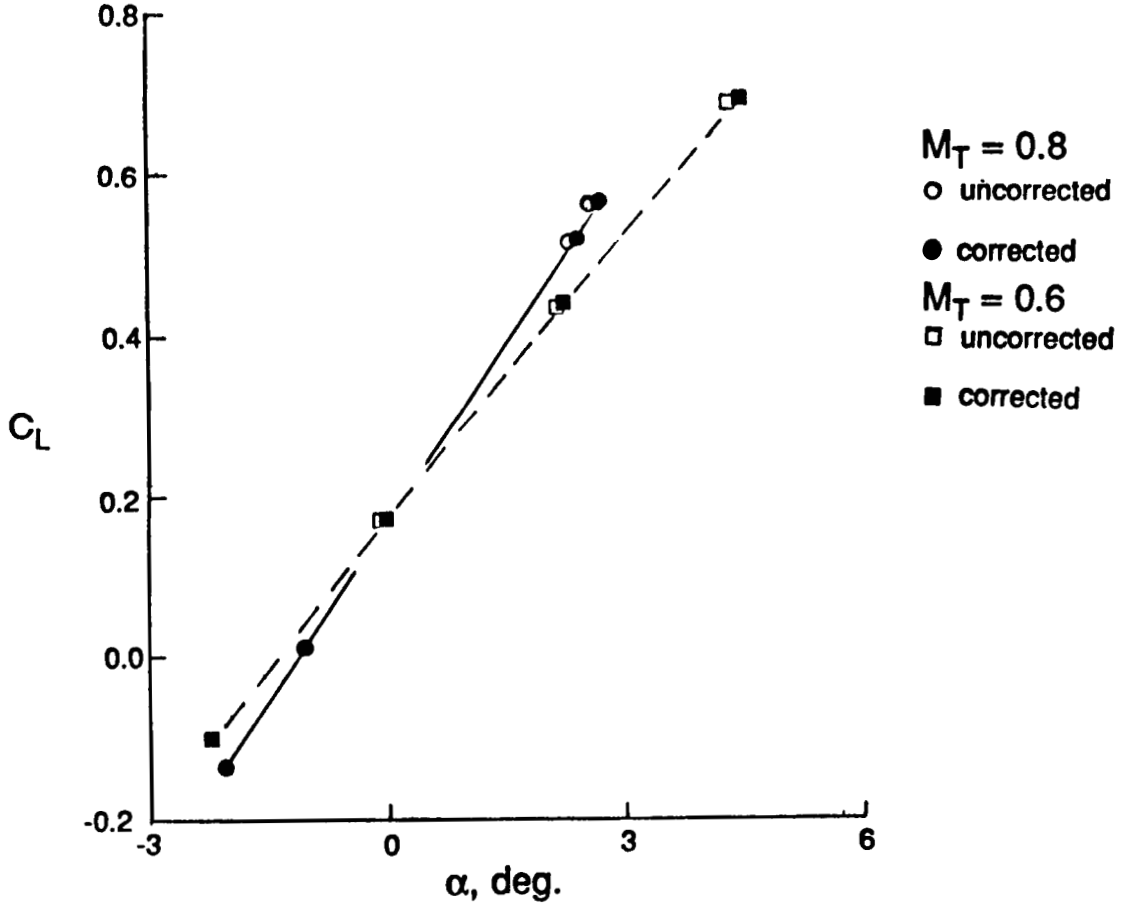

Figure 14. - Sample results for 3-D TUNCOR WIAC application to Pathfinder I data from the NTF; Lift curves at $M_T = 0.6$ and 0.8, $Re_c = 2 \times 10^6$.